UNIVERSITY OF CALIFORNIA SAN DIEGO

Origin of Bajaites from Jaraguay and San Borja Volcanic Fields in Baja California, Mexico

A Thesis submitted in partial satisfaction of the requirements
for the degree of Master of Science

in

Earth Sciences

by

Michelle A. Bibbins

Committee in charge:

Jane Teranes, Chair
Paterno Castillo
Geoffrey Cook
James Day

2018

The Thesis of Michelle A. Bibbins is approved, and it is acceptable in quality and form for publication on microfilm and electronically:

Chair

University of California San Diego

2018

TABLE OF CONTENTS

LIST OF FIGURES

LIST OF FIGURES

LIST OF TABLES

ACKNOWLEDGEMENTS

I would like acknowledge Paterno Castillo for being my advisor throughout this process. Without his expertise and patience, I would not be here today and I would not have been able to go to AGU in 2014. His guidance has proved invaluable to me both academically and professionally.

I would like to also acknowledge James Day for allowing me to do my trace element analysis at SIGL, and for assisting me with my writing. His inputs and guidance have benefitted me tremendously.

I would like to acknowledge Jane Teranes, for taking over chairmanship of the committee. Without her patience, I would not have been able to defend.

I would like to acknowledge Geoffery Cook for recommending me to be his teaching assistant and for being a mentor to me throughout my academic career. Without his guidance, I would not have developed the passion that I now have for Earth Science and for teaching others.

I would like to acknowledge Bernardo Amador-Garcia and Raquel Negrete-Aranda for providing Paterno with the samples and for always answering my emails with questions about the field sampling and ages of the samples.

Lastly, I would like to acknowledge the graduate student body and alumni at Scripps Institution of Oceanography. All of the late night study sessions were really memorable and special to me.

ABSTRACT OF THE THESIS

Origin of Bajaites from Jaraguay and San Borja Volcanic Fields in Baja California, Mexico

by

Michelle A. Bibbins

Master of Science in Earth Sciences

University of California San Diego, 2018

Jane Teranes, Chair

The dynamic tectonic history of peninsular Baja California commenced at approximately 13 Ma, when subduction along the northwestern coast of Mexico ceased. Subsequently, the Gulf of California opened, and transverse faults formed parallel to the ancestral trench. Post-subduction arc-related magmatism continued while the Baja peninsula was forming until approximately one million years ago. The post-subduction lavas that erupted in the peninsula have variable compositions ranging from calc-alkalic to tholeiitic arc basalts. Bajaite is a collective term that describes andesites and basaltic andesites found in Baja California that, like adakites, are characterized by elevated magnesium, silica, and incompatible trace element concentrations. However, in contrast, bajaites exhibit relative enrichment in Sr—their origin is the subject of discussion. It has been proposed as the product of partial melting of subducted oceanic crust - similar to the proposed origin of adakite - or partial melting of the metasomatized mantle wedge due to its arc lava-like features, such as depletion in Nb and Ta, and relative enrichment in Sr. Bajaite has also been proposed as a mixture of differentiated and mafic arc lavas. The composition of bajaite is similar to the bulk continental crust and, thus, its true origin can explain a potential mechanism of continental growth. In this study, I use the petrographic, major and trace element, and Sr-Nd-Pb isotopic data for bajaites from the Jaraguay and San Borja volcanic fields in Baja California Norte, Mexico to show that their source is plausibly the depleted mantle wedge metasomatized by a subduction component.

Introduction

The formation of continental crust is a topic that has fascinated geochemists for many years. It is important most simply because we reside on the crust and precious mineral ores are found within it (Hoffman, 1988). The way that Earth continuously produces and recycles the crust, also known as plate tectonics, has not been observed on any other planets. Evidence for this as well as records of early life is preserved in fossils and zircon crystals found in continental crust (Knoll, 2015; Valley et al., 2014). Geochemists use chemical and isotopic compositions of crustal rocks to constrain their petrogenetic and geochronologic histories, as well as to make thermal models of the Earth. The consensus is that continental crust forms through partial melting of the mantle and is ultimately expressed as intrusive or extrusive igneous rocks (McCulloch and Gamble, 1991; Sawyer, 1994; Kelemen et al., 1993; Patchett et al., 1982; Grove et al., 2012). The majority of continental crust was produced early in the Earth's history, possibly due to higher mantle potential temperature, which facilitated a higher degree of partial melting (Smithies et al., 2003; Cawood et al., 2006; Polat, 2012; Rapp et al., 2003; Taylor and McLennan, 1995). Other models suggest a more uniform (Hurley, 1968) or episodic (McLennan and Taylor, 1982) rate of crustal production via subduction and/or accretion of oceanic material onto the continents (Busby, 2004). Moreover, the Archaean continental crust was produced through a combination of complex episodic events that resulted in various distinct geologic units or assemblages. Among the late Archaean rock assemblages that are of special interest in this study are high-magnesian (high-Mg) granodiorites, which are also known as sanukitoids (Martin, 1994). Previous work has suggested that these rocks were formed through partial melting of hydrated peridotite (Stern et al., 1989) or recycled basaltic crust (Martin et al., 2010).

Presently, researchers who study continental crust formation focus on subduction zones because the interaction of subducted fluids with the overlying mantle wedge causes the mantle solidus to decrease and, thus, mantle to partially melt. Therefore, it is generally accepted that much of the continental crust that is being produced today is through arc magmatism (Hoffman, 1988; Rudnick, 1995). However, continental crust production is less abundant today because the Earth is cooler than during the Archaean (Rudnick, 1995). Age and temperature constraints from oxygen, uranium-lead, and hafnium isotopic data from zircon suggest a hotter mantle in early Earth history (e.g., Dhuime et al., 2012).

High-magnesian andesites (HMA) are thought to be associated with continental crust production because of their compositional similarities with Archaean sanukitoids (Shirey and Hanson, 1984), and with bulk silicate Earth (BSE). However, it should be noted that their MgO contents are significantly lower than those suggested for BSE (Taylor and McLennan, 1985; McDonough and Sun, 1995). High-magnesian andesites are rare arc lavas and are known for their high MgO compositions (>5 wt. %), high Mg# ((Mg/[Mg+Fe]) × 100 >50), as well as low FeO*/MgO ratios (<1, where FeO* is total Fe oxides; Tatsumi et al., 2008; Kelemen, 1995). These are also known as “primitive andesites” (Kelemen et al., 2003) and “high Mg# andesites" (Kelemen, 1995). Many petrogenetic investigations have concluded that HMA lavas can be produced through partial melting of the mantle wedge that has been metasomatized by slab-derived components (i.e., fluids including volatiles) and/or direct slab melts (e.g., Tatsumi, 2006;

Yogodzinski et al., 1998). As noted earlier, it has been proposed that sanukitoids were produced through a similar process (Martin et al., 2005; Stern et al., 1989).

Adakite is another rare subduction zone lava that was originally defined by Defant and Drummond (1990, 1993) to have high SiO_2 (≥ 56 wt. %), Al_2O_3 (≥ 15 wt. %), MgO (>3 to <6 wt. %), Sr (≥ 400 ppm), Y (≤ 18 ppm), Yb (≤ 1.9 ppm), and $^{87}Sr/^{86}Sr$ (< 0.7040) contents. Since then, the formation mechanism for adakites has been debated and, consequently, evolved to cover a range of mechanisms ranging from direct partial melting of subducted basaltic crust (also known as slab melting; Defant and Drummond, 1990, 1993; Saunders et al., 1987), to mixing of felsic and primitive melts (Streck et al., 2007) and to melting of the lower crust (Gao et al., 2004; Chung et al., 2003) or of peridotite metasomatized by melt from subducted basaltic crust (Kay, 1978; Martin et al., 2005). High-magnesian andesites have also been considered adakites (Martin et al., 2005). Additionally, the definition of adakite has evolved to include many compositions. Specifically, high-SiO_2 adakites (HSA) are considered to represent felsic melts from subducted MORB that have subsequently reacted with peridotite during their ascent whereas low silica adakites (LSA) are considered to have formed by melting of a peridotitic mantle wedge that has been modified by reaction with such felsic melts (Martin et al., 2005).

Both adakites and HMA are strongly associated with arc processes; in fact, adakites were named after the location where they were first observed—in Adak Island, located in the Aleutian subduction zone. It is believed that a high supply of water and extra heat to melt the cold slab is needed to produce both HMA and adakites (Grove et al., 2012; Tatsumi, 2006). This heat can come from a young and buoyant subducted ocean crust (Defant and Drummond, 1990), or from an anomalously hot overlying mantle (Kay, 1978). Adakites and rocks with adakitic characteristics (or adakitic rocks), however, occur in many places around the world where arc magmatism is not and/or no longer taking place, including China (Gao et al., 2004; Liu et al., 2014; Kang et al., 2009; 2014), India (Naqvi et al., 2007) and Baja California (Rogers et al., 1985; Saunders et al., 1987, Aguillon-Robles et al., 2001).

Bajaites are Neogene-Quaternary lavas that were erupted after the cessation of subduction in the Baja California peninsula. These are a type of HMA and, hence, display the aforementioned adakitic characteristics, most notably the high Sr/Y ratio because of their high Sr concentration. Due to their adakitic composition and the purported presence of adakites in the Santa Clara volcanic field in Baja California, it had been suggested that bajaites are also a product of slab melting (Aguillon-Robles et al., 2001; Benoit et al., 2002). Several additional explanations have been offered to justify the idea that slab melting is a widespread process contributing to the monogenetic post-subduction volcanism of Baja California, including slab window formation (Aguillón-Robles et al., 2001; Calmus et al., 2011), slab tearing (Pallares et al., 2007) and viscous dissipation due to the shear stress of the adjacent Toscos-Abreojos fault zone (Negrete-Aranda et al., 2013). However, the origin of adakites and adakitic rocks is controversial (e.g., Castillo, 2012 for a summary) and, therefore, the true source of bajaite is investigated.

Geologic Background

The most dominant and oldest rock unit in the Baja California peninsula in northwestern Mexico (Fig. 1) is the Peninsular Ranges Batholith that is Cretaceous in age. This igneous complex has a calc-alkaline origin, indicating that there was active subduction taking place on the western margin of North America since at least 65 Ma. The Peninsular Ranges Batholith is compositionally and temporally heterogeneous in nature and is comprised of two terranes: the Alisitos Arc to the west and the undifferentiated, intrusive La Posta type plutons to the east (Atwater, 1989; Lonsdale, 1991; Silver and Chappell, 1988; Todd et al., 1994; Kimbrough et al., 2001). However, this Cretaceous basement is poorly exposed because it lies beneath numerous younger lava flows. These younger flows consist predominantly of volcanic rocks of the Comondu arc (Hausback, 1984), which is associated with the southern end of the Peninsular Ranges Batholith and was the result of westward migration of the volcanic front (Umhoefer et al., 2003, Castillo, 2008). Since the volcanic front would migrate to the East due to the shallowing of the subduction angle as the subducted lithosphere became younger and, hence, more buoyant (Busby, 2004), the westward migration of the front is not due to arc processes. Activity of the Comondu arc was not uniform throughout the peninsula. It was active from 24 to 11 Ma in the south (Sawlan and Smith, 1984), and from 24 to 16 Ma to the north (Martin-Barajas et al., 2000). Rock outcrops of the Comondu formation indicate that subduction and calc-alkaline volcanism continued until around 12.5 Ma, when spreading segments of the EPR collided with western Mexico (Atwater, 1970; Lonsdale, 1991; Busby et al., 1998). It was initially thought that segments of the EPR that collided with Baja California were subducted

(Saunders et al., 1987; Calmus et al., 2003; Pallares et al., 2007). However, abandoned spreading ridges offshore of southern and central Baja California have been observed, and clearly show that this is not the case (Lonsdale, 1991; Tian et al., 2011). Subsequently, at approximately 12 Ma, a complex transform boundary was formed starting from the northwest, and this resulted in the formation of proto-Gulf of California in the east and Toscos-Abreojos fault zone to the west of the peninsula (Spencer, 1979).

The cessation of subduction in the west and subsequent opening of the Gulf of California in the east at 6 Ma also resulted in large variations in the geochemistry of lavas that were erupted in the peninsula, thus creating one of the densest and largest monogenetic volcanic provinces on the planet (Aguillon-Robles, 2002). Across the peninsula, their compositional varieties include tholeiites, alkali basalts, andesites, trachybasalts, niobium-enriched basalts, adakites, and HMA that, as mentioned earlier, are locally referred to as bajaites (Fig. 1). Spatially, the bajaite outcrops are consistently located to the west of the ancient Commondu arc (Calmus et al., 2003; Pallares et al., 2008). Tholeiites are found mostly in the south of the peninsula and rarely in the north (Bellon et al., 2006). Alkali basalts, trachybasalts, adakites, and niobium-enriched basalts tend to align with the ancient forearc (Aguillon-Robles et al., 2013, 2001; Gastil, 1975; Luhr et al., 1995). This diverse monogenetic volcanism persisted for approximately 12 million years after the cessation of subduction.

Outcrops of bajaites occur predominately in the Jaraguay and San Borja volcanic fields (Fig. 1) together with a variety of post subduction lavas that were erupted since ~13 Ma. The latter include trachybasalts, absarokites, rhyolites, and ignimbrites. The volcanic fields are located in the state of Baja California Norte in Mexico, with Jaraguay being more northerly of the two locales. These two volcanic fields are aligned with the axis of the Commondu arc, which lies to the ~eastern side of the peninsula. In the field, the bajaite outcrops are characterized as blocky sheet flows that were mostly probably erupted from fissures, as very few isolated vents have been observed (Negrete-Aranda et al., 2010). The samples that are examined in this study represent a range rocks that were taken from outcrops in the Jaraguay and San Borja volcanic provinces.

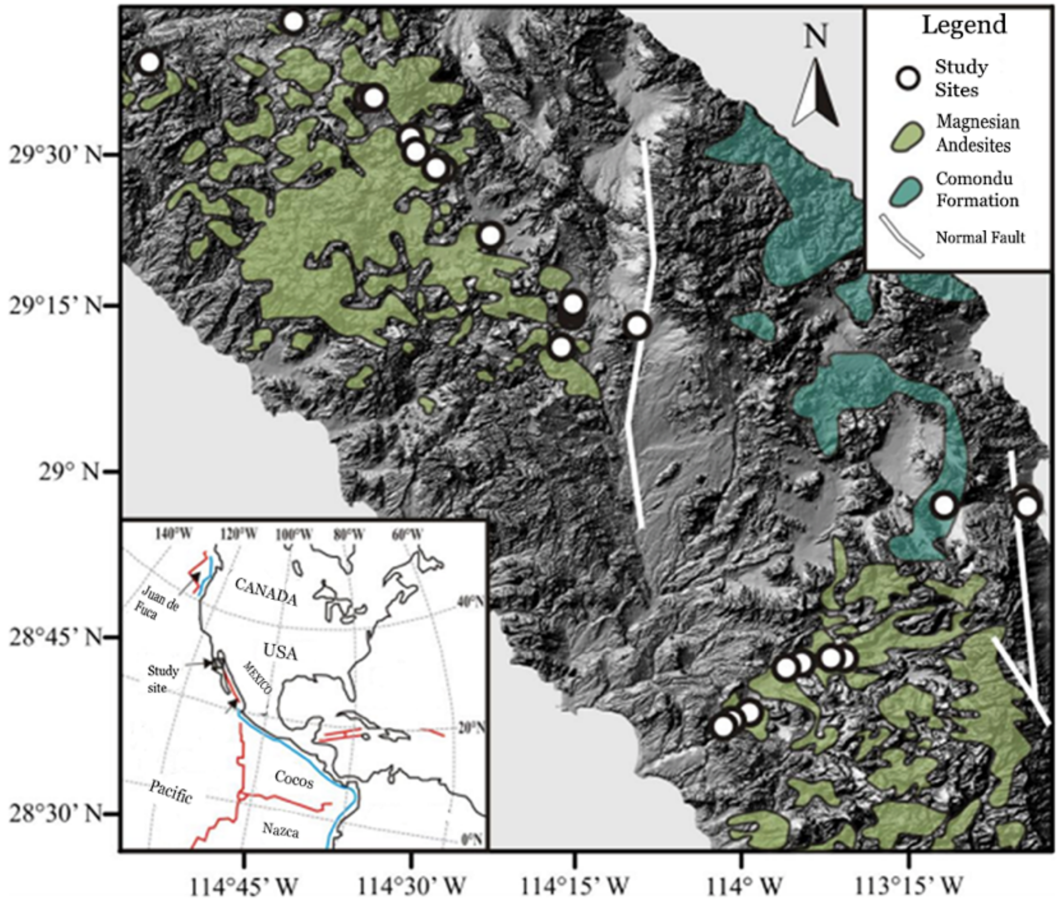

Figure 1: A simplified geologic map of the study area, showing outcrops of bajaites (HMA) and Comondu arc formation, as well as sample locations (white circles). Inset shows the location of the study area. This figure was modified after Garcia-Amador et al. (2012).

Samples and Methods

Samples

Bajaite samples were collected in the field by Raquel Negrete-Aranda, Bernardo Garcia-Amador, and Edgardo Canon-Tapia from roughly between latitudes 28°30’ and 29°45’ in Baja California, Mexico. These were collected primarily for a paleomagnetic study at the Universidad Nacional Autónoma de México (UNAM), and, thus, were taken with a rock drill. All samples were broken into cm-size chips, leached in ~2.5% HNO_3 to eliminate contamination from drilling, and dried at 105 ºC for about 24 - 36 hours in an oven prior to powdering using an alumina ceramic grinding container.

Major elements

Major element measurements were analyzed using X-Ray Fluorescence (XRF) spectrometry at the Washington State University GeoAnalytical Lab (Johnson et al., 1999). The concentrations of elements in the samples were measured by comparing the X-ray intensities of selected elements with the intensities of two beads each of the nine USGS standards (AGV-1, BCR-1, BIR-1, DNC-1, G-2, GSP-1, PCC-1, STM -1 and W-2, using the values recommended by Govindaraju, 1994), in addition to two beads of pure vein quartz that were used as blanks for every element except Si. The 20 standard beads were ran and used for recalibration at an interval of approximately three weeks or after the analysis of about 300 unknown samples. The intensities for every element are automatically corrected for line interference and absorption effects due to presence of other elements using the fundamental parameter method (Johnson et al., 1999). Long-term precision for the XRF analysis is typically <2% (2σ) of the amount present. Loss of ignition (LOI) was analyzed by weighing approximately 1 gram of sample in a quartz crucible and heating it in a furnace at 1000 °C for at least one hour. The sample was then cooled in a vacuum and reweighed. The difference in the sample mass is reported as the LOI value. The major element and LOI data are reported in Table 1 and lab dulicate data is reported in Table A1.

Trace elements

For trace element analysis, approximately 25 mg of powdered sample was digested in a concentrated, double-distilled 2:1 mixture of HF:HNO3 acid inside of a Teflon beaker (Castillo et al., 2014). After digestion, the resulting solutions were spiked with an indium internal standard for the purpose of monitoring instrument drift and sensitivity throughout the run. Diluted solutions were measured on a ThermoScientific iCAP Qc quadropole inductively-coupled plasma mass spectrometer (ICP-MS) using the normal, low-resolution mode at the Scripps Isotope Geochemistry Laboratory (SIGL) at Scripps Institution of Oceanography (SIO; Day et al., 2014). Analyses were standardized against reference materials BCR-2, BHVO-2, and BIR-1, which were measured at various times throughout the analytical run. Reproducibility based on repeated measurements of the reference materials was generally < 3% (RSD) except for Pb, Zn, Rb and Ge, which were <4%, <8%, <15%, and <20%, respectively. The trace element abundance data is reported in Table 2 and lab duplicate data is reported in Table A2.

Isotopes

For Sr, Nd, and Pb isotopic analysis, the samples were digested with double distilled, concentrated 2:1 mixture of $HF:HNO_3$ acid in Teflon beakers. Strontium and rare earth elements (REE) were separated from aliquots of the resulting solutions in ion exchange columns using HCl as the eluent. Then Nd was separated from the rest of the REE in ion exchange columns using 2-hydroxyisobutyric acid as the eluent. Lead was separated from aliquots of the same solutions using small ion exchange columns in a HBr medium. Total procedural blanks are <35 pg for Sr, <80 pg for Nd, and <90 pg for Pb. Strontium, Nd and Pb isotope analyses were performed using a 9-collector, Micromass Sector 54 thermal ionization mass spectrometer at SIO. (Castillo et al., 2014). None of these samples were spiked. Details of the analysis plus accuracy and precision are listed under Table 3.

Results

Petrography

The majority of the sample set have a microcystalline, sparsely to moderately porphyritic (<15% phenocrysts) texture and are moderately vesicular. Olivine with inclusions of spinel is the most abundant phenocryst and has experienced low temperature alteration as evidenced by the presence of iddingsite along edges and fractures. Minor amounts of clinopyroxene and hornblende phenocrysts are also present, but plagioclase phenocrysts are rare. Clinopyroxenes are variably altered and show mild exsolution lamellae and alteration along edges. Hornblendes phenocrysts are also variably altered. The groundmass generally consists of dark glass and microcrystalline olivines; some samples have long, thin, microcrystalline plagioclase in the matrix as well. Accessory minerals include sphene and oxide minerals. These petrographic characteristics approach those of sanukitoids from the Setouchi volcanic belt, southwestern Japan, except the latter have no plagioclase phenocrysts (Tatsumi, 2006).

Major Elements

The major element contents of the samples analyzed are presented in Table 1 and Table A1. In terms of rock chemistry, most of the samples are basaltic andesites (SiO_2 = 52 – 57) and the rest are basalts (SiO_2 = 45-52), andesites (SiO_2 = 57-63), dacites (SiO_2 = 63-77)and rhyolites (SiO_2 = 69 – 77) – one from Jaraguay and two from San Borja although only one was analyzed for major elements (Fig. 2). They have variable compositions (SiO_2 = 46-73%, MgO = 0.2-9.95%, CaO = 1.48 - 9.59%, FeO* = 2 - 8.62%, P_2O_5 = 0.026 - 1.44%, Al_2O_3 = 11.65 - 17.5%, TiO_2 = 0.13 - 3.38%, MnO = 0.04 - 0.13%, Na_2O = 2.80- 4.69%, and K_2O = 3.87 - 4.69%). These compositions fall within the range of those previously reported by Saunders et al. (1987) and Calmus et al. (2003). Despite the large compositional variations of the samples, these are collectively referred to as bajaite samples throughout the discussion as they were collected from the same region and, as will be shown below, they are all petrogenetically related to a common source.

Most of the samples fall in the mid-K to high-K fields of Peccerillo and Taylor (1976), with San Borja lavas being richer in K than Jaraguay lavas. In terms of total alkalis (Na_2O + K_2O) versus silica (TAS) classification scheme, the majority of the samples fall in the alkalic field, with only five samples (including the two rhyolites analyzed) in the sub-alkalic or tholeiitic field. Any classification scheme based on K_2O and Na_2O, however, should be taken with caution because if these rocks have undergone alteration or metasomatism, then the method of classifying samples based on alkali contents may not be appropriate (Le Bas et al., 1985). Significantly, the majority of the samples are calc-alkalic based on their FeO*/MgO contents (Miyashiro, 1974). Thus, most of the samples belong to the typical calc-alkaline lava series in a continental convergent margin setting (Kelemen, 1995; Busby, 2004).

The rhyolites have major element compositions that are similar to high-silica adakites from Tonga (Falloon et al., 2008), Tibet (Guo et al., 2007), Ecuador (Chiaradia et al., 2009), and India (Naqvi et al., 2007). As stated earlier, adakites are a subset of arc volcanic rocks that were originally proposed to be melts derived from subducted MORB (Defant and Drummond, 1990, 1993). Over the years, however, the definition of adakite has been expanded to include both low and high silica varieties (Martin et al., 2005). High silica adakites have more andesitic to rhyolitic SiO_2 compositions, 4-8% CaO +Na_2O, less than 1%TiO_2, and <15 Nb, <1500 Sr. Low silica adakites have more basseltic-andesistic composition, and can be more enriched in Nb and Sr.

Table 1: Major element composition of bajaites from Baja California, Mexico.

Sample	Location	SiO_2	TiO_2	Al_2O_3	FeO*	MnO	MgO	CaO	Na_2O	K_2O	P_2O_5	Sum
12B007A	San Borja	51.08	1.69	13.52	6.39	0.09	7.62	8.93	2.80	3.60	0.42	96.14
12B018B	San Borja	51.68	1.65	13.84	6.62	0.12	6.75	8.62	2.98	4.00	0.71	96.97
12B023B	San Borja	51.73	1.61	14.16	6.36	0.09	7.58	8.41	2.81	3.78	0.54	97.07
12B033B	San Borja	47.20	3.38	12.16	8.62	0.12	7.09	8.38	3.00	2.33	1.17	93.44
12B039C	San Borja	50.74	1.47	15.82	7.59	0.13	6.25	8.54	3.26	2.90	0.49	97.19
12B057B	San Borja	46.15	2.69	11.65	8.18	0.10	8.59	9.59	3.23	3.01	1.44	94.63
12B062B	San Borja	51.70	1.75	13.90	6.85	0.10	5.78	9.05	3.60	3.05	0.72	96.51
12B080C	San Borja	72.79	0.27	13.21	2.00	0.04	0.54	1.48	3.44	4.63	0.03	98.42
12B087C	San Borja	56.40	0.80	16.66	6.04	0.10	5.51	7.29	3.35	1.76	0.21	98.13
12B107C	Jaraguay	53.59	2.07	15.67	6.29	0.09	5.78	8.09	4.33	2.19	0.53	98.62
12B116A	Jaraguay	53.21	2.00	15.57	6.19	0.08	6.06	8.15	4.29	2.07	0.46	98.09
12B123B	Jaraguay	53.72	2.02	15.75	6.31	0.09	6.00	7.96	4.39	2.14	0.55	98.94
12B145B	Jaraguay	53.94	0.69	15.47	5.67	0.10	8.57	7.38	4.44	1.29	0.19	97.74
12B153B	Jaraguay	52.50	0.70	17.47	6.42	0.12	8.03	8.85	3.84	1.00	0.17	99.09
12B161B	Jaraguay	52.55	0.70	17.50	6.44	0.12	7.85	8.85	3.85	1.05	0.17	99.08
12B172B	Jaraguay	52.67	0.72	17.44	6.48	0.12	7.76	8.75	3.89	1.05	0.19	99.08
12B180D	Jaraguay	51.49	1.92	15.22	7.59	0.10	5.44	8.19	4.19	2.04	0.42	96.59
12B189A	Jaraguay	72.91	0.13	13.99	2.23	0.04	0.20	1.64	3.87	3.74	0.03	98.76
12B202D	Jaraguay	50.97	1.60	14.54	7.80	0.11	8.60	8.43	4.69	1.43	0.34	98.52
12B226C	Jaraguay	50.49	1.00	15.06	7.21	0.12	9.95	8.46	3.94	1.48	0.52	98.24

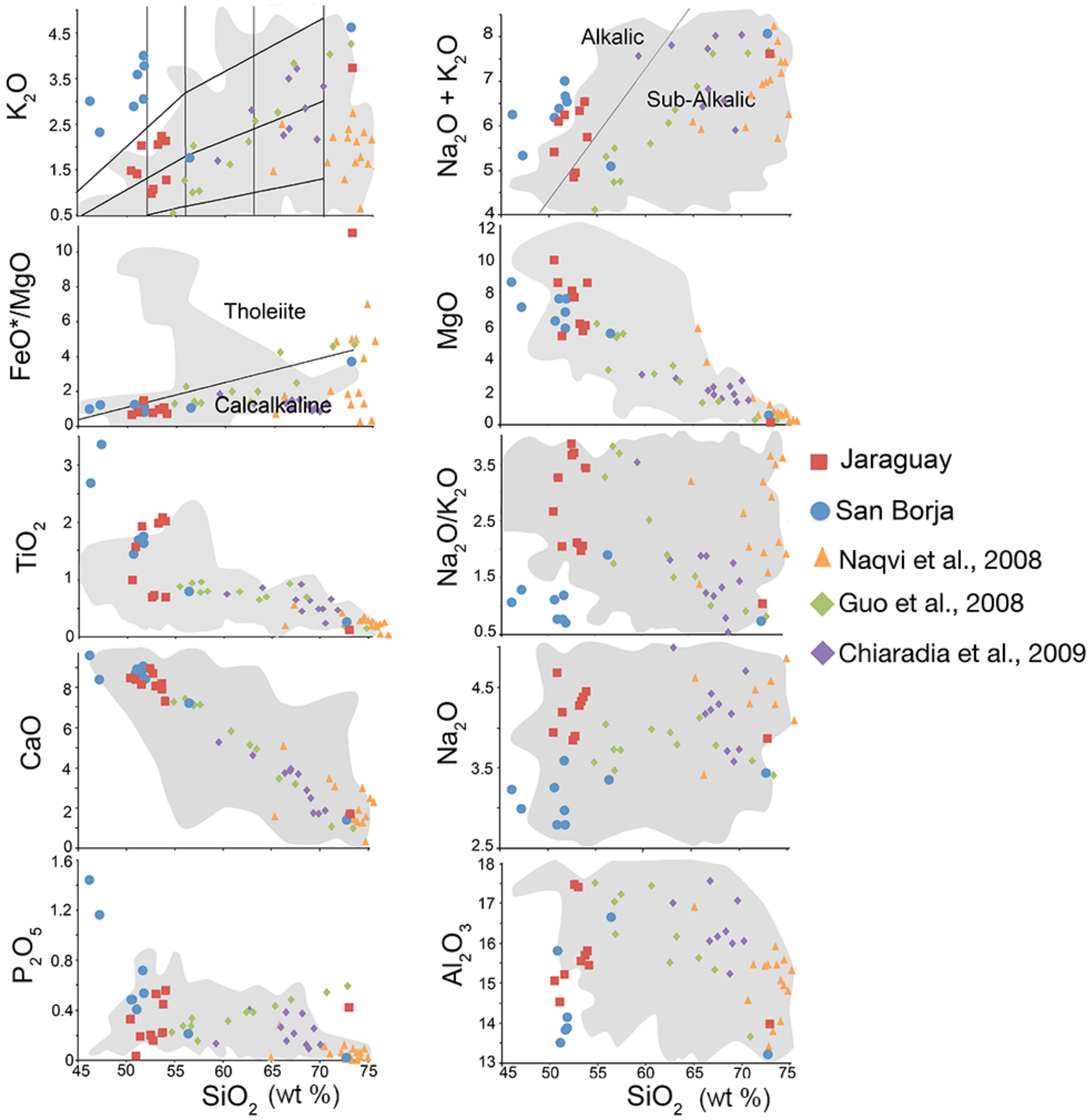

Figure 2: Plots of SiO_2 versus major oxide concentrations and ratios (Harker diagrams - Harker, 1909) for bajaites from Baja California, Mexico. Blue circles represent samples from San Borja and red squares are from Jaraguay. Green diamonds represent Guo et al., 2008. Orange triangles represent Naqvi et al., 2008. Purple diamonds represent Chiaradia et al., 2009. The field for global adakites (source literature citations are listed in bibliography), in grey, is shown for reference.

Bajaites have been suggested to be related to melting of subducted oceanic crust (MORB) (Saunders et al., 1987; Aguillon-Robles et al., 2001; Benoit et al., 2002; Calmus et al., 2011). In this case, bajaites are proposed to be LSA that were formed through melting of the mantle wedge metasomatized by slab melt beneath the peninsula after subduction ceased 12.5 Ma. Thus, both types of adakite appear to be present in Baja California. The major element variations of the samples analyzed indeed match those expected from both adakite varieties (Martin et al., 2005), with rhyolites plotting with HSA and bajaites plotting with LSA. That is, the samples fall within the appropriate LSA and HSA fields in SiO_2 versus Nb, and CaO + Na_2O versus Sr diagrams (Figs. 3a and b). In the TiO_2 versus Cr/Ni diagram, however, most of the samples plot in the overlap of the two fields (Fig 3c). Jaraguay samples consistently plot more inside the adakite field than San Borja in the majority of major element variation plots (Fig. 2).

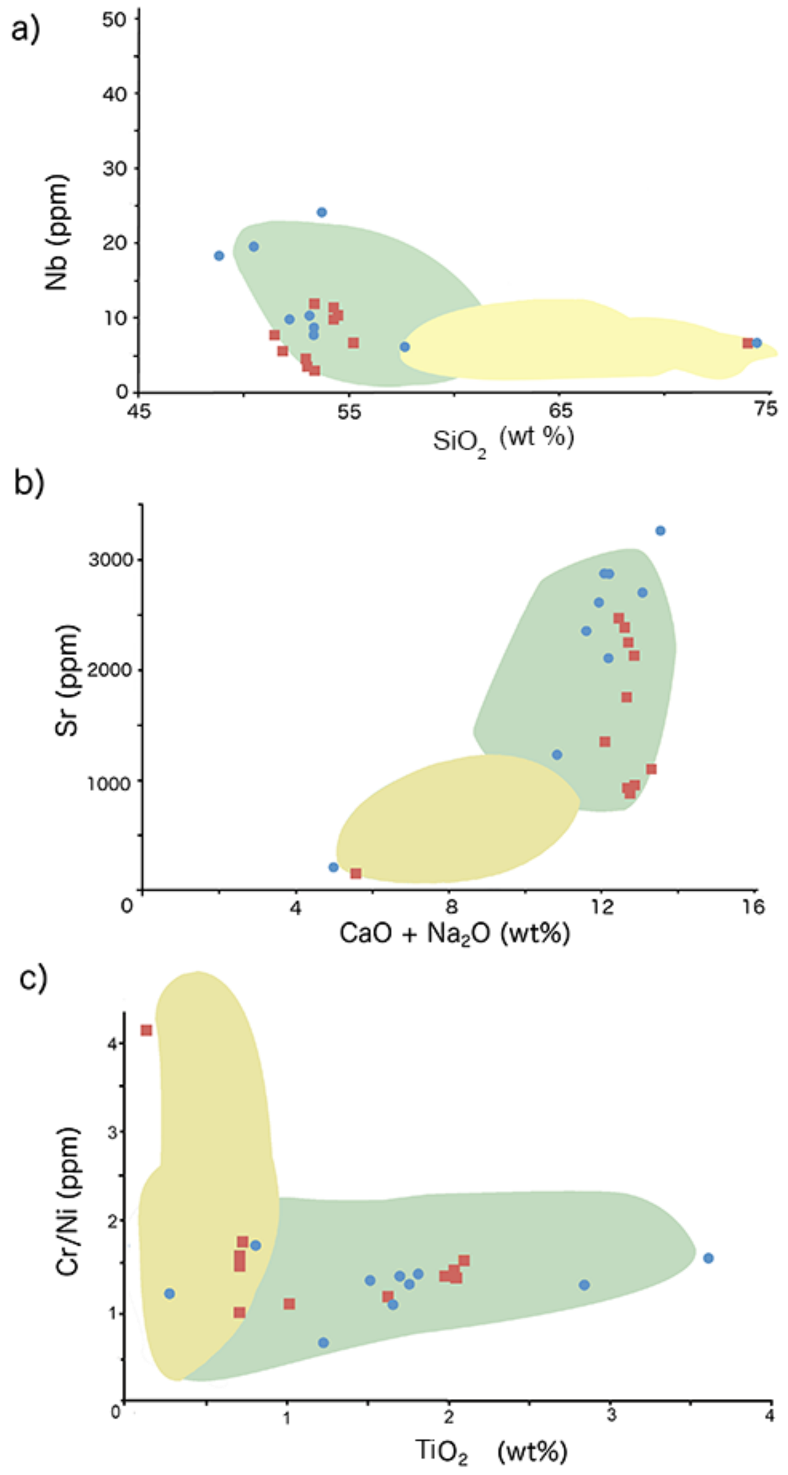

Figure 3: Plots of a) Nb versus SiO_2, b) CaO + Na_2O versus Sr and c) TiO_2 versus Cr/Ni for representative San Borja and Jaraguay bajaites. Yellow and green fields are high and low silica adakites, respectively; modified after Martin et al. (2005). Symbols as in Figure 2.

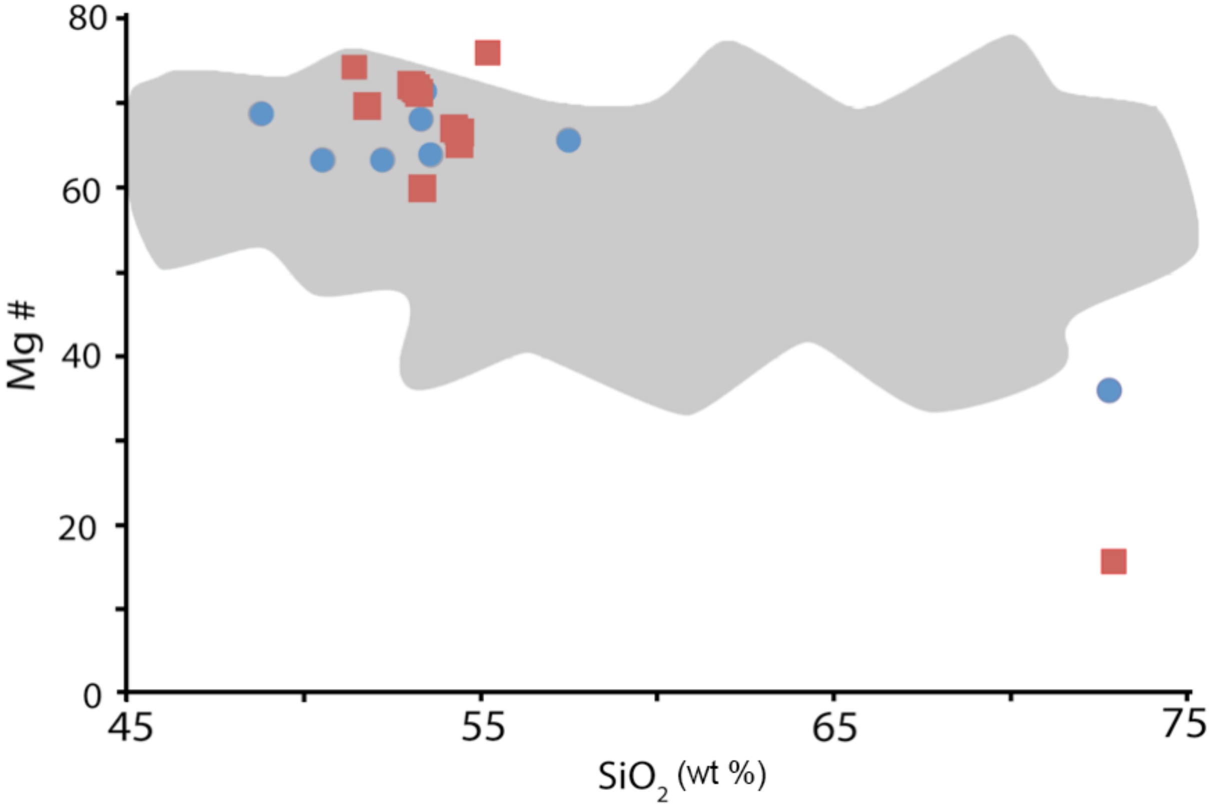

Figure 4: Mg# = (Mg/Mg+Fe)*100 vs SiO_2 contents for representative San Borja and Jaraguay bajaites. Symbols as in Figure 2. The field for global adakites (source literature citations are listed in bibliography), in grey, is shown for reference.

Trace Elements

The trace element contents of the samples are presented in Table 2 and Table A2. Their primitive mantle-normalized (McDonough and Sun, 1995) concentration patterns (Fig. 5) show that in general, all the samples are enriched in highly incompatible relative to moderately-incompatible trace elements. The samples are significantly enriched in Ba (490–3026 ppm), Pb (4.2-22.4 ppm) and Sr (154-3267 ppm), but are depleted in high field-strength elements (HFSE) Nb (2.4-24ppm) and Ta (0.14-1.37ppm) and heavy REE. The bajaites share these general characteristics - positive Ba, Sr, and Pb anomalies, negative Nb and Ta anomalies and relative depletion in heavy rare REE - with other arc calc-alkaline lavas from many places that include, but are not limited to, Oregon (Streck et al., 2007), Mexico (Wallace and Carmichael, 1992), Philippines (Castillo et al., 2008), Italy (De Astis et al., 2000), and other subduction zones from around the world (e.g., Patagonia, Japan, the Marianas, Costa Rica).

The samples also show a clear grouping between the two volcanic fields although there is some degree of overlap. Overall, San Borja volcanics are more enriched in incompatible trace elements than Jaraguay, consistent with the former being more alkaline than the latter. A few samples are noteworthy because their trace element patterns differ from the majority of the samples (Fig. 5). San Borja rhyolites have the highest Rb and Th contents, are slightly enriched in Ta, and are slightly depleted in Ba concentration anomalies. They also have significant positive Pb anomalies by virtue of their lack of positive Sr anomalies. Moreover, they are relatively depleted from Sm to Dy but have relatively normal Y to Lu contents when compared to other samples. The rhyolite from Jaraguay (sample 12B189A) does not have a negative Ba anomaly unlike

Table 2: Trace element composition of bajaites from Baja California.

Sample ID	Location	Li	Sc	Ti	V	Cr	Co	Ni	Cu	Zn	Ga
12B007A	San Borja	8.4	27.4	11881.7	219.7	329.6	36.6	250.7	69.0	126.7	22.6
12B018B	San Borja	8.8	26.7	10267.0	199.7	323.0	37.5	230.2	61.8	110.6	21.2
12B023B	San Borja	7.1	22.2	9351.0	167.0	238.2	32.0	221.2	59.0	108.1	19.5
12B033B	San Borja	7.4	16.6	17085.9	247.9	293.9	30.8	183.1	32.5	136.5	19.1
12B039C	San Borja	6.8	26.5	8682.9	144.0	336.3	36.9	248.1	49.9	108.4	18.3
12B051A	San Borja	7.7	20.0	7703.5	169.5	328.0	31.6	223.5	53.4	101.7	19.7
12B057B	San Borja	11.6	24.6	16129.7	208.8	301.0	34.5	231.5	61.0	181.6	24.2
12B062B	San Borja	9.5	19.2	10830.5	183.7	350.7	34.9	245.3	61.3	120.4	22.2
12B071C	San Borja	38.2	5.5	1643.2	31.6	10.8	3.7	6.2	8.7	69.7	14.0
12B080C	San Borja	27.1	5.7	1216.2	23.1	8.2	3.8	6.8	8.8	58.0	14.2
12B087C	San Borja	14.3	27.8	6046.4	186.6	252.9	31.4	144.3	40.8	121.4	25.5
12B094D	San Borja	12.8	16.3	6009.2	115.1	281.9	25.5	195.5	26.4	116.2	21.0
12B103C	Jaraguay	11.4	20.2	3230.0	124.8	251.5	27.2	200.4	38.3	86.6	18.0
12B107C	Jaraguay	10.8	17.8	12027.7	174.6	194.8	22.1	123.7	35.8	106.4	22.7
12B116A	Jaraguay	9.4	15.8	11532.9	175.1	188.0	22.3	128.8	28.7	127.8	21.6
12B123B	Jaraguay	11.0	34.0	12181.7	184.3	180.5	23.2	129.7	35.3	113.1	23.1
12B133A	Jaraguay	10.4	22.3	13438.7	249.2	179.6	28.9	91.1	30.7	133.7	21.1
12B145B	Jaraguay	8.8	15.5	4063.2	89.2	281.6	29.8	279.2	52.1	102.4	18.0
12B153B	Jaraguay	8.5	26.2	4087.9	186.9	259.9	31.9	169.5	33.3	100.6	16.5
12B161B	Jaraguay	8.2	24.1	3931.4	156.4	250.3	30.9	153.5	65.9	110.1	16.9
12B172B	Jaraguay	8.27	24.2	3721.0	170.1	259.0	31.4	144.9	52.9	77.1	17.1
12B180D	Jaraguay	11.9	18.0	11397.4	207.1	174.7	28.9	124.6	49.6	131.6	22.8
12B189A	Jaraguay	25.9	3.2	758.4	1.4	4.0	1.3	1.0	3.5	81.6	18.1
12B202D	Jaraguay	7.0	12.9	7075.7	152.9	196.8	28.4	167.3	49.7	103.7	14.6
12B207A	Jaraguay	11.4	24.8	16161.5	299.2	215.2	36.0	114.0	36.4	162.0	25.9
12B222C	Jaraguay	9.7	20.1	9620.8	155.5	141.1	21.7	106.8	47.6	105.7	20.8
12B226C	Jaraguay	12.6	22.4	6126.5	174.9	328.1	38.6	301.9	62.6	124.8	19.9
AGV 1 **	Oregon	11.4	12.6	6232.0	119.1	10.4	15.8	18.4	64.9	124.1	20.3
JB1A ***	Japan	11.9	28.0	7564.3	200.8	350.4	38.0	140.5	56.7	129.0	17.3

** USGS recommended values from Smith, 1995.
*** Recommended values from Imai et al., 1995.

Table 2: Trace element concentration in ppm for samples from Baja California (continued).

Sample ID	Ge	Rb	Sr	Y	Zr	Nb	Cs	Ba	La	Ce	Pr	Nd
12B007A	1.8	44.6	2868.9	12.3	427.8	10.2	0.3	3025.8	41.8	97.8	13.1	52.6
12B018B	2.0	30.0	2624.3	17.1	376.9	8.2	0.3	2701.8	50.6	117.4	16.4	66.4
12B023B	1.7	34.2	2341.7	11.4	371.0	7.8	0.3	2228.6	39.7	93.5	12.2	48.3
12B033B	1.7	11.5	2095.9	11.7	226.8	19.1	0.1	759.9	41.2	101.6	13.9	55.8
12B039C	1.8	21.5	2867.9	16.6	339.2	9.7	0.2	1907.3	36.6	90.2	12.0	47.1
12B051A	1.6	19.0	2527.5	13.2	236.6	6.8	0.2	1442.0	41.3	94.3	12.5	49.8
12B057B	2.8	18.2	3266.6	23.0	387.0	17.9	0.2	1559.3	94.3	231.2	31.6	126.5
12B062B	1.9	14.8	2702.4	13.3	297.7	23.6	0.2	1669.9	49.2	115.7	15.4	61.2
12B071C	0.7	152.5	404.1	11.2	66.0	8.7	4.5	1146.8	29.3	52.7	5.2	16.0
12B080C	0.7	167.2	206.0	9.6	58.1	6.5	5.6	1216.7	31.7	56.3	5.6	17.0
12B087C	1.5	44.3	1216.6	20.6	189.4	5.9	2.1	1042.6	26.4	58.4	7.8	32.2
12B094D	1.4	24.5	1760.9	12.2	229.1	8.0	0.3	1432.8	39.9	84.6	9.9	36.4
12B103C	0.9	12.2	883.8	6.9	94.0	2.4	0.5	569.9	8.8	18.3	2.3	9.0
12B107C	1.5	17.4	2391.1	10.6	257.0	10.5	0.1	1379.1	34.9	80.3	10.6	42.0
12B116A	1.3	14.1	2254.6	9.5	235.5	10.0	0.1	1315.7	30.0	69.7	9.0	35.3
12B123B	1.6	16.6	2449.0	11.1	255.7	10.8	0.2	1412.8	37.9	87.0	11.4	44.8
12B133A	1.4	8.8	1512.9	9.6	135.2	8.3	0.2	715.1	13.1	30.8	4.1	17.4
12B145B	0.9	10.4	1341.0	9.2	128.1	6.5	0.2	860.1	16.6	35.6	4.2	16.3
12B153B	1.1	7.4	900.0	10.6	96.8	3.9	0.2	662.3	10.8	23.5	3.0	12.0
12B161B	1.0	8.9	938.6	11.9	93.6	3.4	0.1	679.4	12.2	26.0	3.3	13.6
12B172B	1.1	9.0	938.6	12.3	90.4	2.8	0.1	694.2	13.4	28.7	3.6	14.8
12B180D	1.5	12.8	2123.8	9.5	173.2	11.7	0.3	1722.6	25.6	60.4	7.6	30.0
12B189A	1.1	111.8	154.1	29.0	65.7	6.6	2.8	1187.4	28.8	58.3	6.8	25.1
12B202D	1.0	6.4	1102.4	7.5	96.7	5.3	0.1	490.4	15.4	35.8	4.7	18.7
12B207A	1.8	10.0	1843.9	15.3	163.9	10.1	0.3	975.6	21.7	51.1	6.9	28.6
12B222C	1.1	8.7	1979.2	7.6	180.1	6.2	0.3	869.1	19.5	46.0	6.2	26.0
12B226C	1.5	7.8	1752.6	13.1	132.2	7.2	0.1	1187.9	34.6	75.5	9.5	35.8
AGV 1 **	1.4	67.5	678.9	20.0	237.8	14.4	1.3	1245.8	39.6	72.0	8.7	33.1
JB1A ***	1.5	37.2	448.7	22.6	136.4	27.6	1.2	506.7	37.9	66.8	7.2	26.6

** USGS recommended values from Smith, 1995.
*** Recommended values from Imai et al., 1995.

Table 2: Trace element concentration in ppm for samples from Baja California (continued).

Sample ID	**Sm**	**Eu**	**Gd**	**Tb**	**Dy**	**Ho**	**Er**	**Tm**	**Yb**	**Lu**	**Hf**	**Ta**	**W**	**Pb**	**Th**	**U**
12B007A	8.0	3.0	6.5	0.6	2.6	0.5	1.3	0.1	1.0	0.1	11.0	0.5	0.4	21.1	6.9	1.9
12B018B	10.7	3.4	8.6	0.8	3.4	0.6	1.6	0.2	1.1	0.2	9.9	0.4	0.3	22.4	8.2	1.9
12B023B	7.6	2.7	6.1	0.6	2.5	0.4	1.2	0.1	0.9	0.1	9.2	0.4	0.2	20.0	7.4	1.6
12B033B	8.6	2.4	6.6	0.6	2.7	0.4	1.1	0.1	0.8	0.1	5.3	0.9	0.2	6.1	3.5	1.0
12B039C	7.3	2.6	6.2	0.7	3.3	0.6	1.8	0.3	1.6	0.2	8.7	0.5	0.4	20.8	5.5	1.5
12B051A	8.1	2.4	6.4	0.7	2.8	0.5	1.4	0.2	1.0	0.1	5.6	0.3	0.2	14.4	5.5	1.4
12B057B	20.4	4.8	15.7	1.5	5.8	0.9	2.2	0.2	1.3	0.2	8.9	0.9	0.4	12.0	10.0	2.8
12B062B	9.8	2.8	7.6	0.7	3.0	0.5	1.3	0.2	0.9	0.1	7.6	1.4	0.2	14.1	5.4	1.3
12B071C	2.4	0.8	2.6	0.3	1.7	0.3	1.1	0.2	1.2	0.2	2.3	0.8	0.9	17.8	20.5	5.7
12B080C	2.5	0.8	2.6	0.3	1.6	0.3	1.0	0.2	1.1	0.2	2.1	0.7	0.9	18.7	22.1	4.1
12B087C	6.4	2.1	6.0	0.8	4.0	0.8	2.0	0.3	1.8	0.3	5.2	0.3	0.8	11.4	6.9	2.1
12B094D	5.6	1.9	5.0	0.5	2.4	0.4	1.2	0.2	1.0	0.1	5.4	0.4	0.3	14.0	10.4	1.8
12B103C	1.7	0.8	1.6	0.2	1.3	0.3	0.7	0.1	0.7	0.1	2.4	0.1	0.2	6.6	2.0	0.6
12B107C	6.5	2.3	5.3	0.5	2.5	0.4	1.1	0.1	0.8	0.1	5.9	0.5	0.2	10.7	5.1	1.1
12B116A	5.8	2.0	4.7	0.5	2.1	0.4	0.9	0.1	0.7	0.1	5.4	0.5	0.2	12.8	4.6	1.0
12B123B	6.9	2.3	5.6	0.6	2.5	0.4	1.1	0.1	0.8	0.1	6.1	0.6	0.3	11.1	5.5	1.3
12B133A	3.3	1.5	3.0	0.4	2.1	0.4	1.0	0.1	0.8	0.1	3.4	0.4	0.2	6.6	1.9	0.5
12B145B	2.9	1.1	2.7	0.3	1.8	0.3	1.0	0.1	0.9	0.1	3.2	0.3	0.4	9.6	2.2	0.5
12B153B	2.3	1.1	2.3	0.3	1.9	0.4	1.1	0.2	1.1	0.2	2.4	0.2	0.2	5.0	1.3	0.4
12B161B	2.6	1.1	2.6	0.3	2.0	0.4	1.2	0.2	1.3	0.2	2.4	0.2	0.1	4.2	1.3	0.4
12B172B	2.8	1.2	2.7	0.4	2.1	0.4	1.3	0.2	1.3	0.2	2.1	0.2	0.1	4.9	1.4	0.4
12B180D	4.9	1.8	4.1	0.5	2.1	0.3	1.0	0.1	0.7	0.1	4.4	0.6	0.2	11.7	3.4	0.9
12B189A	4.8	1.3	4.9	0.7	4.6	1.0	2.8	0.4	2.6	0.3	1.9	0.6	0.2	8.1	10.3	2.2
12B202D	3.0	1.0	2.8	0.3	1.5	0.3	0.8	0.1	0.6	0.1	2.6	0.3	0.2	5.5	1.7	0.6
12B207A	5.5	2.1	4.9	0.6	3.2	0.5	1.5	0.2	1.1	0.2	4.1	0.5	0.3	7.7	2.5	0.6
12B222C	4.5	1.7	3.6	0.4	1.7	0.3	0.8	0.1	0.6	0.1	4.3	0.3	0.2	7.3	1.6	0.6
12B226C	5.7	1.8	5.1	0.5	2.5	0.5	1.3	0.2	1.2	0.2	3.3	0.4	0.1	10.0	3.4	0.7
AGV 1 **	6.0	2.0	6.0	0.7	3.7	0.7	2.0	0.3	1.7	0.2	5.3	0.9	0.7	36.3	6.5	1.9
JB1A ***	5.2	1.6	5.4	0.7	4.2	0.8	2.3	0.3	2.1	0.3	3.6	1.7	2.6	6.2	9.1	1.6

** USGS recommended values from Smith, 1995.

*** Recommended values from Imai et al., 1995.

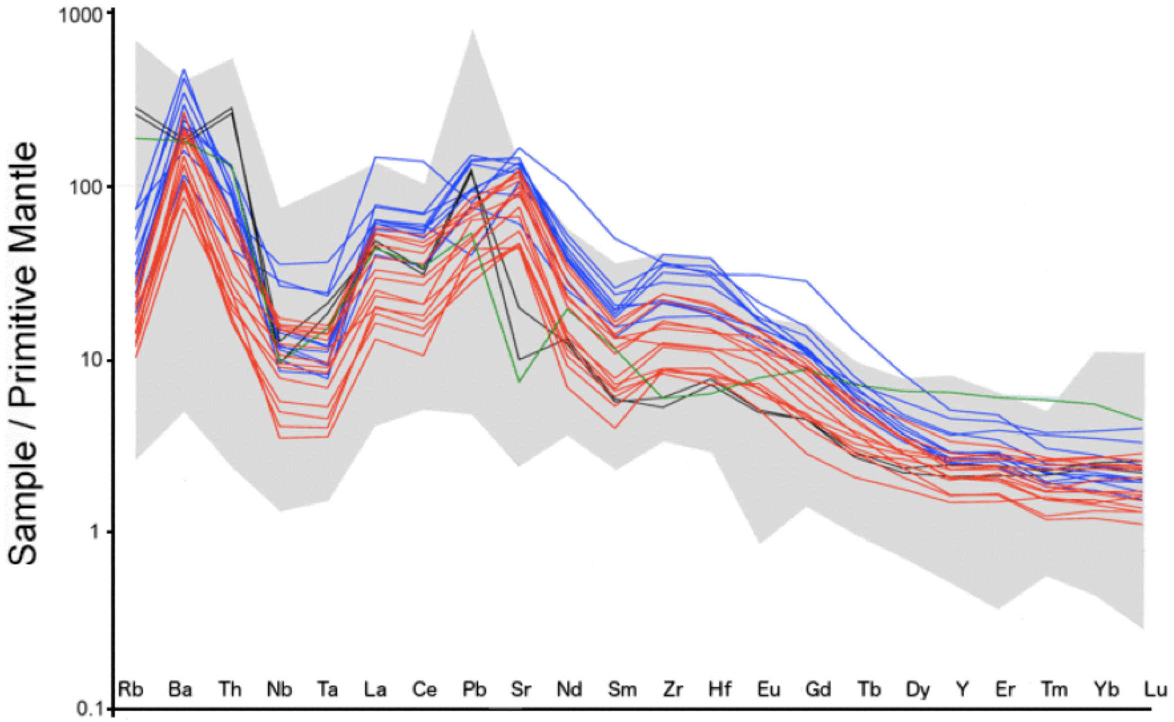

Figure 5: Trace element concentrations of San Borja and Jaraguay bajaites, normalized to the primitive mantle values of McDonough and Sun (1995). Red represents basaltic lavas and green represents rhyolite from Jaraguay. Blue represents basaltic lavas and black represents rhyolites from San Borja. The field for global adakites (source literature citations are listed in bibliography), in grey, is shown for comparison.

the rhyolites from San Borja, has a pronounced negative Sr anomaly and is enriched in moderately incompatible elements Gd to Lu. Finally, a basaltic andesite from Jaraguay (sample 12B057A) is highly enriched in La to Y, displaying the highest light- to middle-REE concentrations among the samples.

Most of the San Borja and some of the Jaraguay samples fall within the adakite field in the La/Yb versus La plot (Fig. 6A; after Defant and Drummond 1990). In contrast, most of the Jaraguay samples and only a few San Borja samples plot in the adakite field in the Sr/Y versus Y plot (Fig. 6b), as in the case for major elements (Fig. 2). Most of the San Borja samples have higher Y and higher Sr/Y ratio for given Y concentration than adakites. This is consistent with the most significant feature of bajaite; it has high Sr content as evidenced by their distinctive positive Sr concentration anomalies in the spider diagram (Fig. 5; see also Table 2 and Table A2). Overall, the bajaites are more enriched in incompatible trace elements like Ba and Zr than most adakites with similar SiO_2 concentrations (Fig. 7). Furthermore, the bajaites show notable enrichments in Co and Ni, but similar Cr and V, when compared with other adakites from around the world.

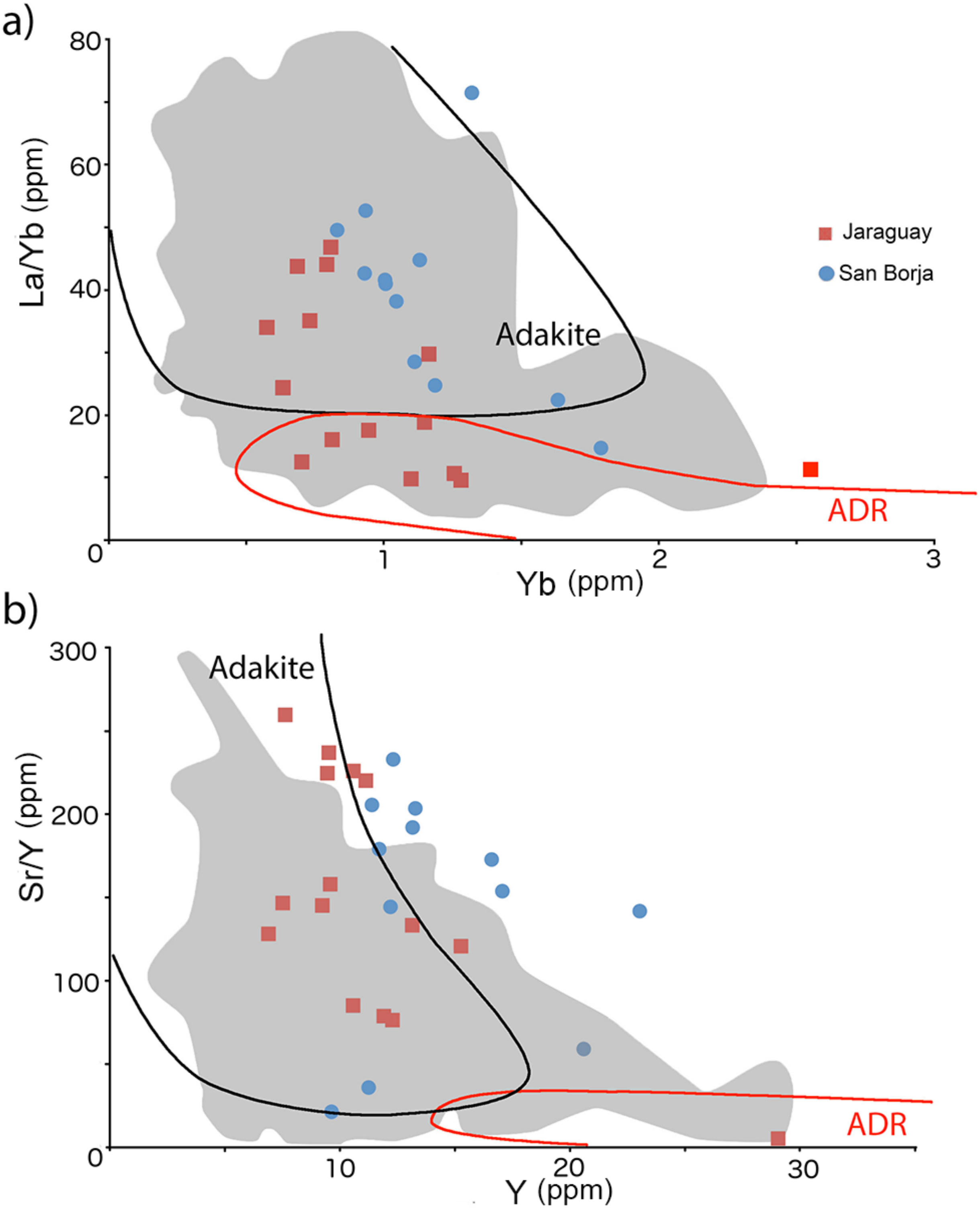

Figure 6: a) La/Yb versus. Yb and b) Sr/Y versus Y for San Borja and Jaraguay bajaites. Diagrams modified after Defant and Drummond, 1990. Symbols as in Figure 2. The field for global adakites (source literature citations are listed in bibliography), in grey, is shown for reference.

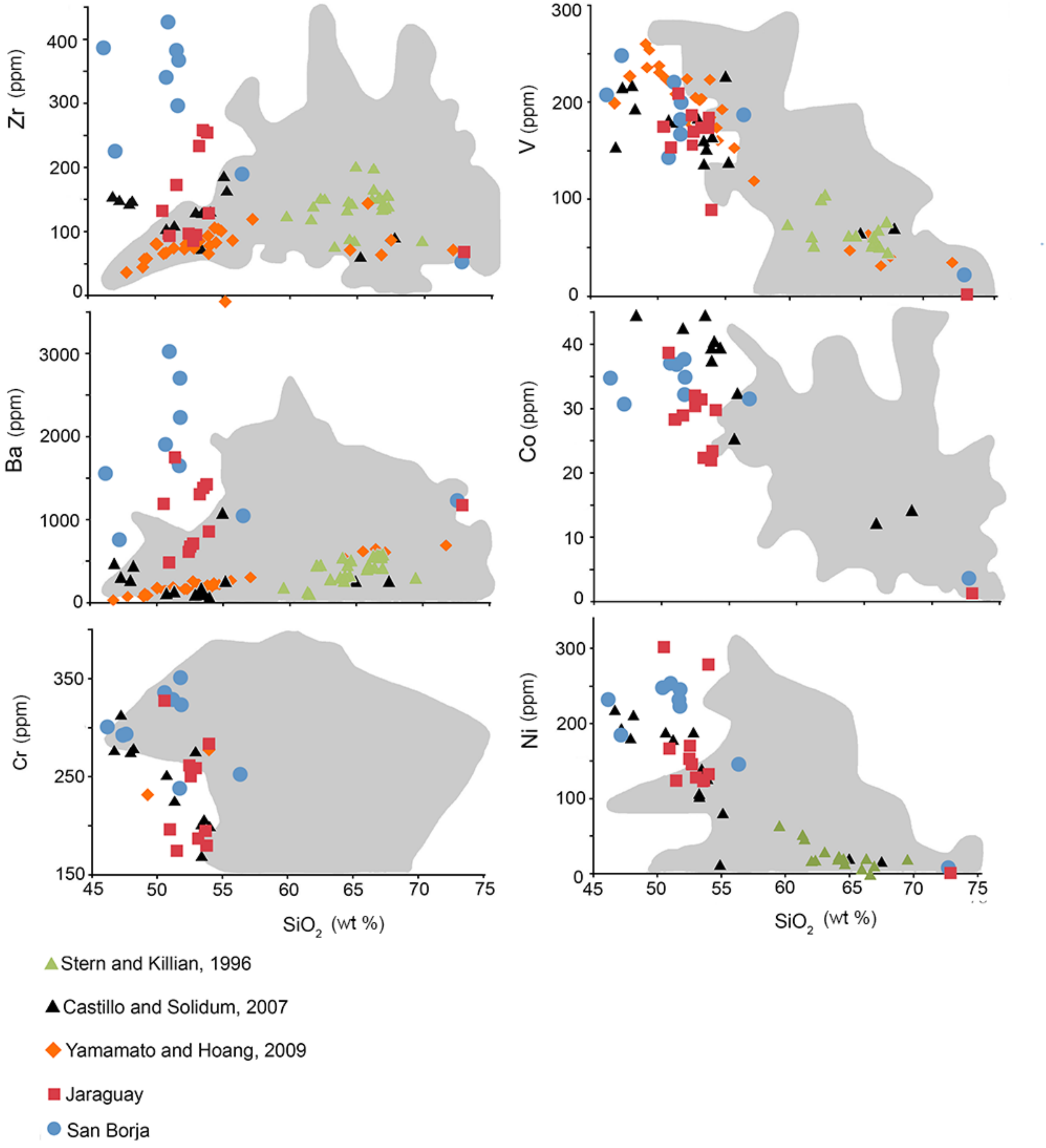

Figure 7: Plots of select trace elements versus SiO₂ for San Borja and Jaraguay bajaites. Data for adakites from other locales are also shown. Black triangles represent Castillo and Solidum, 2007. Green triangles represent Stern and Killian, 1996. Orange diamonds represent Yamamato and Hoang, 2009. The field for global adakites (source literature citations are listed in bibliography), in grey, is shown for reference. Symbols as in Figure 2.

Sr-Nd-Pb Isotopic Ratios

The Sr, Nd and Pb isotopic ratios of representative Baja California samples are presented in Table 3. The samples have variable $^{87}Sr/^{86}Sr$ (0.703703 - 0.704943) and $^{143}Nd/^{144}Nd$ (0.512725 - 0.512865) values (Fig. 8). Lead isotopic values are also variable ($^{206}Pb/^{204}Pb$ = 18.719-18.787; $^{207}Pb/^{204}Pb$ = 15.558-15.603; $^{208}Pb/^{204}Pb$ = 38.382 - 38.565; Fig. 9). The new $^{87}Sr/^{86}Sr$ and $^{143}Nd/^{144}Nd$ overlap with previous values for bajaites and calc-alkaline rocks from Baja California (Rogers et al., 1989; Benoit et al., 2002), and samples from the Trans-Mexican Volcanic Belt (TMVB; Benoit et al., 2002; Aguillón-Robles et al., 2001; Verma, 1984, 1989, 1991, 2000, 2001; Cebria et al., 2011). They also partly overlap with samples from both the Setouchi Volcanic Belt in Japan (Shimoda et al., 1998) and Southern Volcanic Zone (SVZ; Holm et al. 2014; Lopez-Escobar et al., 1995). The samples cluster according to their geographic areas, with Jaraguay samples being depleted in Sr, and enriched in Nd versus the San Borja samples. However, these isotopic values are different than those for MORB from the southern EPR ($^{87}Sr/^{86}Sr$ = 0.7024-0.7035; $^{143}Nd/^{144}Nd$ = 0.5129-0.51335; Castillo et al., 2000) and Baja adakites ($^{87}Sr/^{86}Sr$ = 0.7031-0.7035; $^{143}Nd/^{144}Nd$ = 0.5130-0.51314; Aguillon-Robles et al., 2001). The bajaites have slightly higher $^{143}Nd/^{144}Nd$ but lower $^{87}Sr/^{86}Sr$ than the BSE ($^{143}Nd/^{144}Nd$ = 0.512638; $^{87}Sr/^{86}Sr$ = 0.7045).

Table 3: Sr, Nd and Pb isotopic compositions of bajaites from Baja California, Mexico.

San Borja

Sample	^{87}Sr/^{86}Sr	2σ	^{143}Nd/^{144}Nd	2σ	^{206}Pb/^{204}Pb	^{207}Pb/^{204}Pb	^{208}Pb/^{204}Pb
12B007A	0.704033	7	0.512781	9	18.733	15.597	38.539
12B007A(D)	-		0.512762	10	-	-	-
12B023B	0.704055	7	0.512771	11	18.778	15.603	38.565
12B087C	0.704943	9	0.512736	8	18.719	15.558	38.339
12B087C(D1)	-		0.512733	14	-	-	-
12B087C(D2)	-		0.512725	14	-	-	-

Jaraguay

Sample	^{87}Sr/^{86}Sr	2σ	^{143}Nd/^{144}Nd	2σ	^{206}Pb/^{204}Pb	^{207}Pb/^{204}Pb	^{208}Pb/^{204}Pb
12B116A	0.703791	9	0.512851	6	18.742	15.581	38.425
12B116A(D)	-		0.512865	7	-	-	-
12B145B	0.703696	7	0.51283	7	18.754	15.577	38.405
12B172B	0.703703	9	0.512845	7	18.722	15.579	38.382
12B202D	0.703828	8	0.512784	8	18.787	15.581	38.446
12B226C	0.703909	10	0.512818	6	18.736	15.584	38.425

Strontium isotopic ratios were measured through dynamic multi-collection and fractionation corrected to ^{87}Sr/^{86}Sr = 0.1194. Repeated measurements of NBS 987 yielded ^{87}Sr/^{86}Sr = 0.710256 ± 0.000017 (n=18); 2σ indicates in-run precisions. Neodymium isotopic ratios were measured in oxide form through dynamic multi-collection and fractionation corrected to ^{143}NdO/^{144}NdO = 0.72225 (^{143}Nd/^{144}Nd = 0.7219). Repeated measurements of the La Jolla Nd Standard yielded ^{143}Nd/^{144}Nd = 0.511856 ± 0.000010 (n=17). Lead isotopic ratios were measured through static multi-collection mode. The measured values were then fractionation-corrected off-line using the repeated measurements of NBS SRM 981 (n=22; 206Pb/204Pb=16.899 ± 0.007, 207Pb/204Pb = 15.445 ± 0.010, and 208Pb/204Pb = 35.550 ± 0.026) relative to those of Todt et al., 1996 (206Pb/204Pb=16.9356, 207Pb/204Pb = 15.4891, and 208Pb/204Pb = 36.7006). (D) means duplicate run on the same bead.

The samples do not segregate by volcanic field in the Pb-Pb isotopic diagrams (Fig. 9), unlike in the $^{87}Sr/^{86}Sr$ versus $^{143}Nd/^{144}Nd$ diagram, because the San Borja samples cover the entire range of the Jaraguay samples. However, one San Borja sample (12B087C) with the most depleted $^{206}Pb/^{204}Pb$, $^{207}Pb/^{204}Pb$ and $^{208}Pb/^{204}Pb$ is the most enriched in terms of $^{87}Sr/^{86}Sr$ and $^{143}Nd/^{144}Nd$. Overall, samples from San Borja are more radiogenic in Sr and Pb isotopes but less radiogenic in Nd isotopes than those from Jaraguay. The new $^{206}Pb/^{204}Pb$, at least, overlap with previous values for bajaites, alkaline (including niobium enriched) basalts and tholeiites from Baja California (Rogers et al., 1989; Benoit et al., 2002), and samples from the TMVB (Benoit et al., 2002; Aguillón-Robles et al., 2001; Verma, 1984, 1989, 1991, 2000, 2001; Cebria et al., 2011).

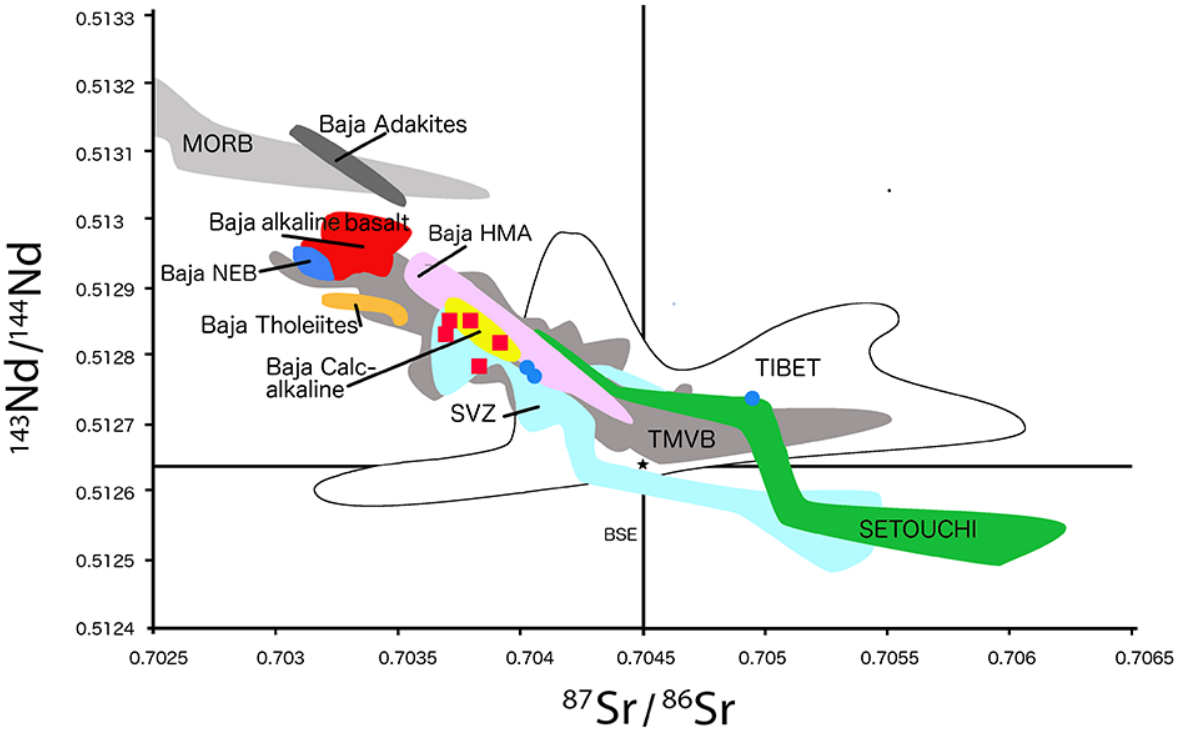

Figure 8: $^{87}Sr/^{86}Sr$ versus $^{143}Nd/^{144}Nd$ for representative San Borja and Jaraguay bajaites. Symbols as in Figure 2. Fields for Baja California tholeiites, and calc-alkaline lavas are from Benoit et al. (2002) and Rogers et al. (1989); Baja California adakites and niobium enriched basalts (NEB) are from Aguillón-Robles et al. (2001); Baja California alkaline basalts are from Storey et al. (1989) and Luhr et al. (1995); Setouchi volcanic field data are from Shimoda et al. (1998); SVZ data are from Holm et al. (2014) and Lopez-Escobar et al. (1995); HMA from Baja are from Rogers et al. (1989) and Aguillon-Robles et al. (2001); MORB is from Castillo et al. (2000); Trans-Mexican Volcanic Belt (TMVB) data is from Verma (1984, 1989, 1991, 2000, and 2001), Cebria et al. (2011), and Garcia-Palomo et al. (2004); Tibet data are from Kang et al. (2009, 2014), and Liu et al. (2014).

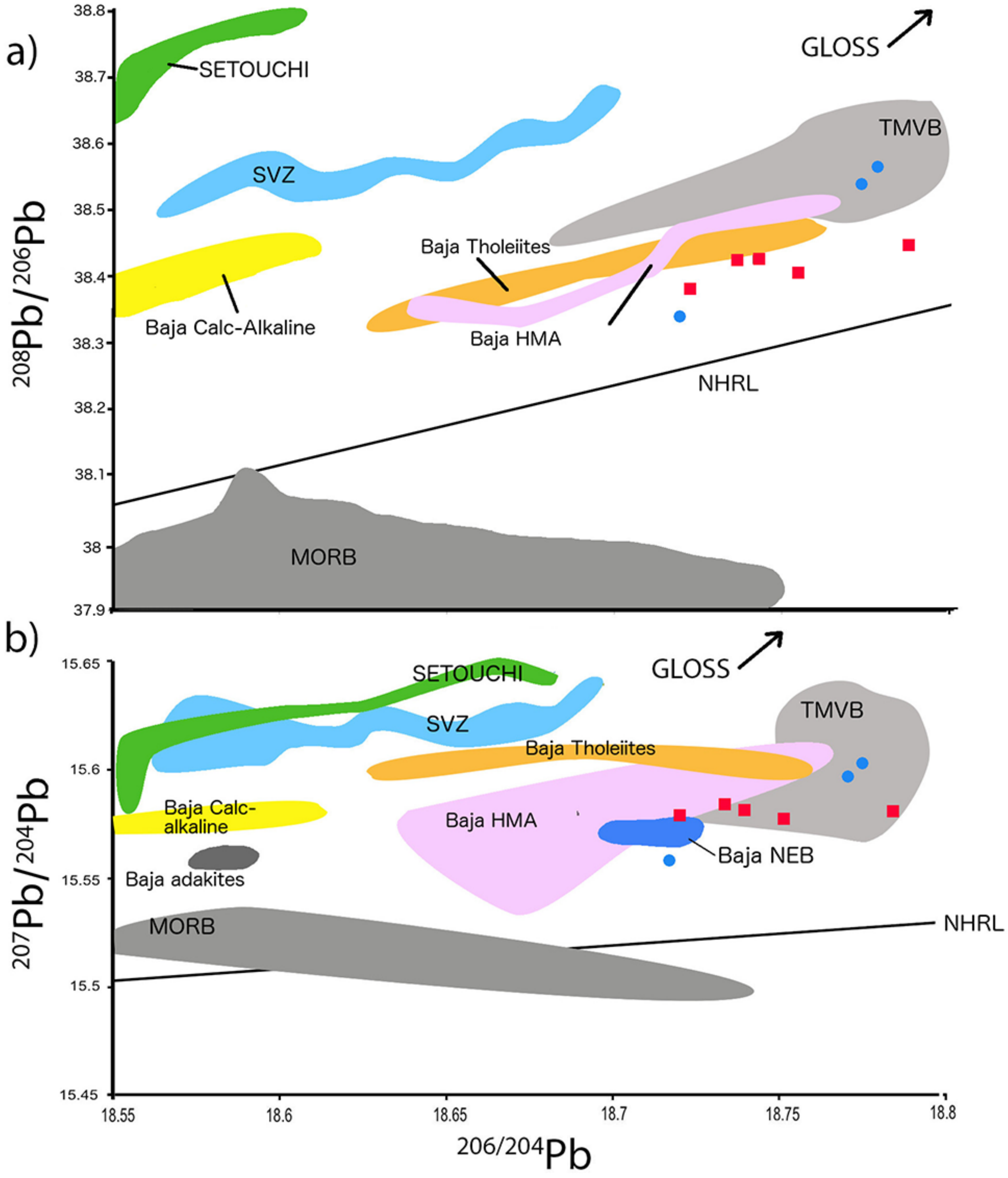

Figure 9: a) ^{206}Pb/^{204}Pb versus ^{208}Pb/^{204}Pb; and b) ^{206}Pb/^{204}Pb versus ^{207}Pb/^{204}Pb whole rock isotopic compositions of representative San Borja and Jaraguay bajaites. Adakites and niobiumm enriched basalts (NEB) from Baja California do not appear in a) because there were no ^{208}Pb/^{204}Pb data available (Aguillon-Robles et al., 2001). Alkaline lavas had too high ^{206}Pb/^{204}Pb values to appear in this figure (Storey et al., 1989, Luhr et al., 1995). Symbols as in Figure 2. Sources of data as in Figure 8.

Discussion

The Baja California samples analyzed in this study display three types of compositional variation that will be discussed and clarified in this section. First, they range from basalt to rhyolite that display major and trace element compositional variations, including varying degrees of differentiation based on their SiO_2 and Mg# values as well as variable trace element concentrations (Table 1, Table A1; Figs. 2, 4, 7). These variations are typical of many volcanic lava suites and, as presented below, can be explained through fractional crystallization. However, although a number of them can be considered quite primitive lavas (e.g., high Mg# and Cr around 300 ppm; Table 1, Table A1, and Figs. 4, 5, 7) that suffer only minor modifications after coming from the mantle (e.g., Wilson, 1989), the fractional crystallization process cannot be modeled quantitatively due to the absence of mineral composition data and lavas with intermediate compositions.

Second, there is a small but generally systematic compositional difference between Jaraguay and San Borja bajaites. This compositional difference between the two sample sites could be explained by source heterogeneity (Warren, 2016). As the bajaites are a type of high magnesium andesite, or primitive andesites (Kelemen et al., 1995, 2003) and more specifically, have a number of primitive compositions, these compositions suggest they were derived from a portion of the metasomatized mantle wedge. These alternative explanations are also discussed below, leading to the third and final type of compositional variation, i.e., trace element and Sr-Nd-Pb isotopic compositional variation that constrains the mantle source of bajaites and, thus, their most probable origin.

The bajaites, which were erupted post-subduction along the northwestern margin of Mexico at ca. 13 Ma until ca. 1 Ma, display significant incompatible trace element and Sr-Nd-Pb isotopic variations that clearly indicate compositional heterogeneity of their mantle source. The heterogeneous mantle source of bajaites is the mantle wedge, similar to that of global arc lavas. However, the dynamic tectonic history that shaped Baja California over the last ~25 million years is atypical for a convergent margin and has left a heterogeneous, residual mantle wedge beneath the peninsula. Partial melting of this residual mantle wedge produced the bajaites, in addition to many other post-subduction, arc-related lavas.

A major implication of this conclusion is that the aforementioned subdivision of the differentiated rhyolites into the HSA field and more mafic bajaite samples to the LSA field does not mean that bajaites are true adakites, because much of the sampels plot in the overlap between high and low silica adakites, respectively. High-SiO_2 adakites (HSA) are considered to represent felsic melts from subducted MORB that have subsequently reacted with peridotite during their ascent whereas low silica adakites (LSA) are considered to have formed by melting of a peridotitic mantle wedge that has been modified by reaction with such felsic melts.

That is, the former are most likely related to the latter simply through fractional crystallization, and not due to interaction with MORB melts. If the subdivision of these samples were true HSA and LSA, then the samples should fall into their expected groups in Figure 3c, rather than plotting in the overlap of the two fields. In Figures 3a and 3b, the samples actually do not fall neatly into those respective subdivisions due to

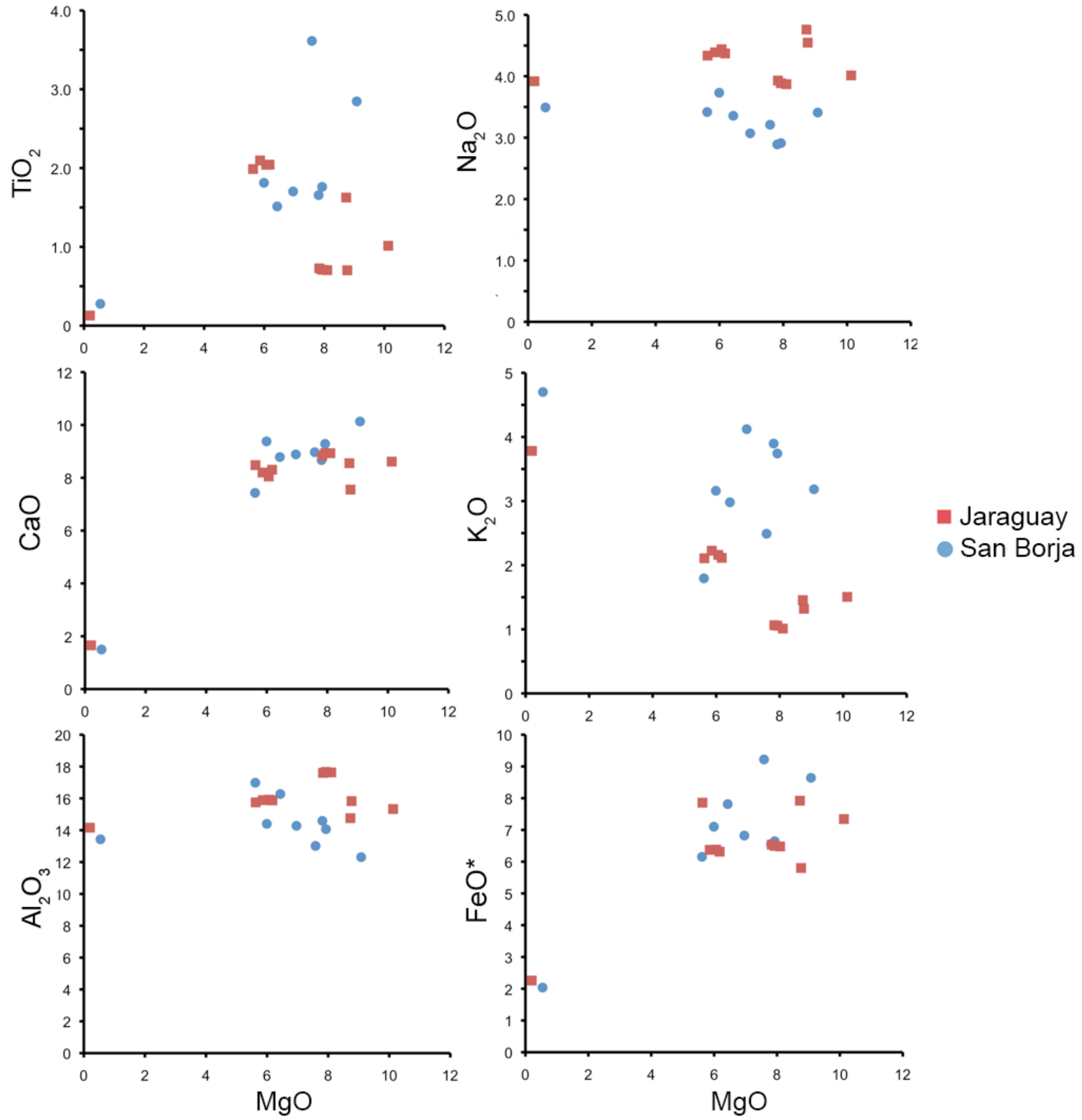

Figure 10: Plots of MgO versus major oxide wt (%) for bajaites from Baja California, Mexico. Symbols as in Figure 2.

melting of MORB, but rather due to crystal separation (i.e., fractional crystallization) of minerals containing major oxides within the magma chamber.

The basalt to rhyolite trend of the samples

The lavas that sit atop the Baja California peninsula have a striking variety of compositions that fall within tholeiitic, calc-alkalic, alkalic, and even shoshonitic lava series that typically display differentiation trends from mafic parents to silicic differentiates (Table 2, Table A2; Tardy et al., 1994; Pallares et al., 2007; Conley et al., 2005). Specifically, the TiO_2, CaO, MgO and Al_2O_3 concentrations decrease wheras FeO*/MgO and Na_2O + K_2O increase as the SiO_2 concentration increases in the samples analyzed in this study (Fig. 2). Moreover, their compatible trace elements V, Co, Ni, and Cr decrease as SiO_2 increases (Fig. 7). These compositional trends are generally interpreted to be the result of fractional crystallization. Fractional crystallization occurs due to crystal separation (e.g., sinking or floating of crystalline material) as the magma cools over time (Bowen, 1922). Therefore, e.g., the increase in SiO_2 is from the loss of Fe and Mg rich minerals as they crystalize (Fig. 2).

The effect of fractional crystallization is shown by plots of MgO versus other oxides (Fig. 10). As in Figure 2, both the San Borja and Jaraguay bajaite suites display differentiation trends, from high MgO to low MgO, that are consistent with fractional crystallization. For example, TiO_2 and Al_2O_3 initially increase and then decrease whereas CaO and FeO* consistently decrease with decreasing MgO. However, their concentrations of TiO_2, CaO, Al_2O_3 and FeO* more or less overlap, indicating that they may indeed have a common, but not identical source. The effects of fractional crystallization on San Borja and Jaraguay bajaites are also shown by the decrease of the trace elements Ni, Co and Cr, which are often found in minerals in primitive melts, such as olivine and pyroxene, with decreasing MgO (Fig. 11). Note that San Borja bajaites are consistently enriched in these elements save for two Jaraguay bajaites that have the highest Ni concentrations. The two bajaite suites differ most in their Zr and Pb concentrations, again indicating that these two volcanic fields were not formed from identical sources and/or melting event.

Temporal Evolution

Another geochemical parameter that may prove useful in constraining the mantle source of bajaites is their temporal evolution. The MgO and select trace element concentrations of bajaites have changed over time, as shown in Figure 12, utilizing ^{40}K-^{40}Ar radiomentric age data published from various studies of these rock formations by Gastil et al., 1979, Saunders et al., 1987, Aguillon-Robles 2002, Calmus et al., 2003, Pallares et al., 2007, Pallares et al., 2008. Overall, the samples have overlapping values, indicating that there is no systematic compositional evolution. Note that the San Borja bajaites are more enriched in compatible trace element concentrations which suggests that they came from a higher degree of partial melt (Blatt et al., 2006), as previously shown in Figures 3, 5 and 7. Moreover, the rhyolites, though limited in occurrence, are not temporally restricted, and as also noted earlier most probably originated through fractional crystallization of more primitive bajaites. Their occurrence may indicate the complex fractionation processes that took place beneath or within the crust. In detail, most of the samples are < 6 Ma, and assuming no sampling bias, may indicate that both San Borja and Jaraguay volcanic fields became more volcanically active at this time. After 6 Ma, the compositions of both bajaite suites became more variable than the older lavas. Moreover, trace element concentrations appear to have decreased in Jaraguay while Sr concentrations increased in San Borja, although both their MgO contents remain similar. What this may indicate is that the San Borja and Jaraguay bajaites have indeed been derived from a heterogenous mantle source and then experienced similar, though physically separated fractional crystallization paths. The source and magmatic differentiation process that affect the bajaites will be discussed in more detail below.

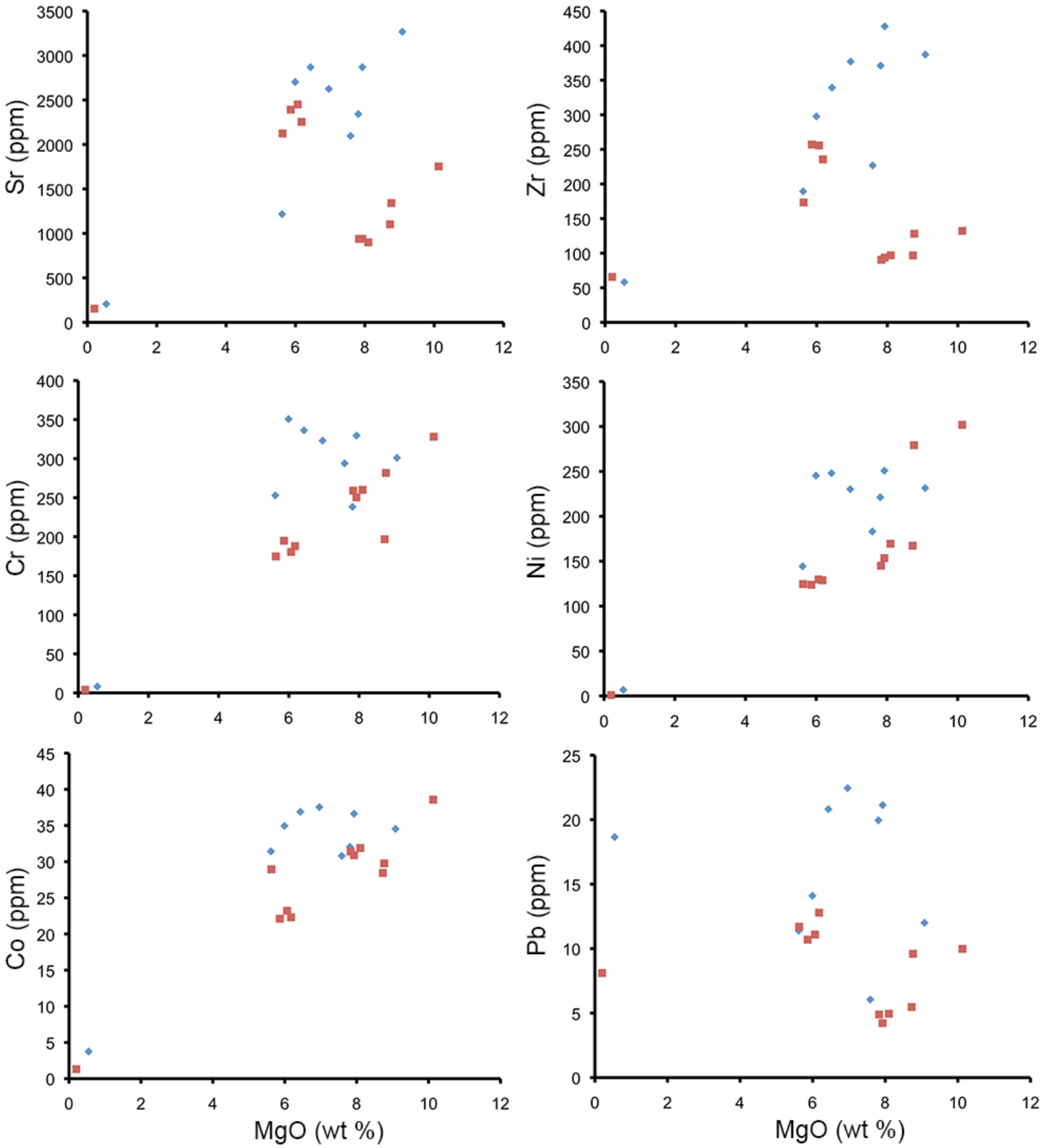

Figure 11: Plots of MgO (wt%) versus select trace elements (ppm) for bajaites from Baja California, Mexico. Symbols as in Figure 2.

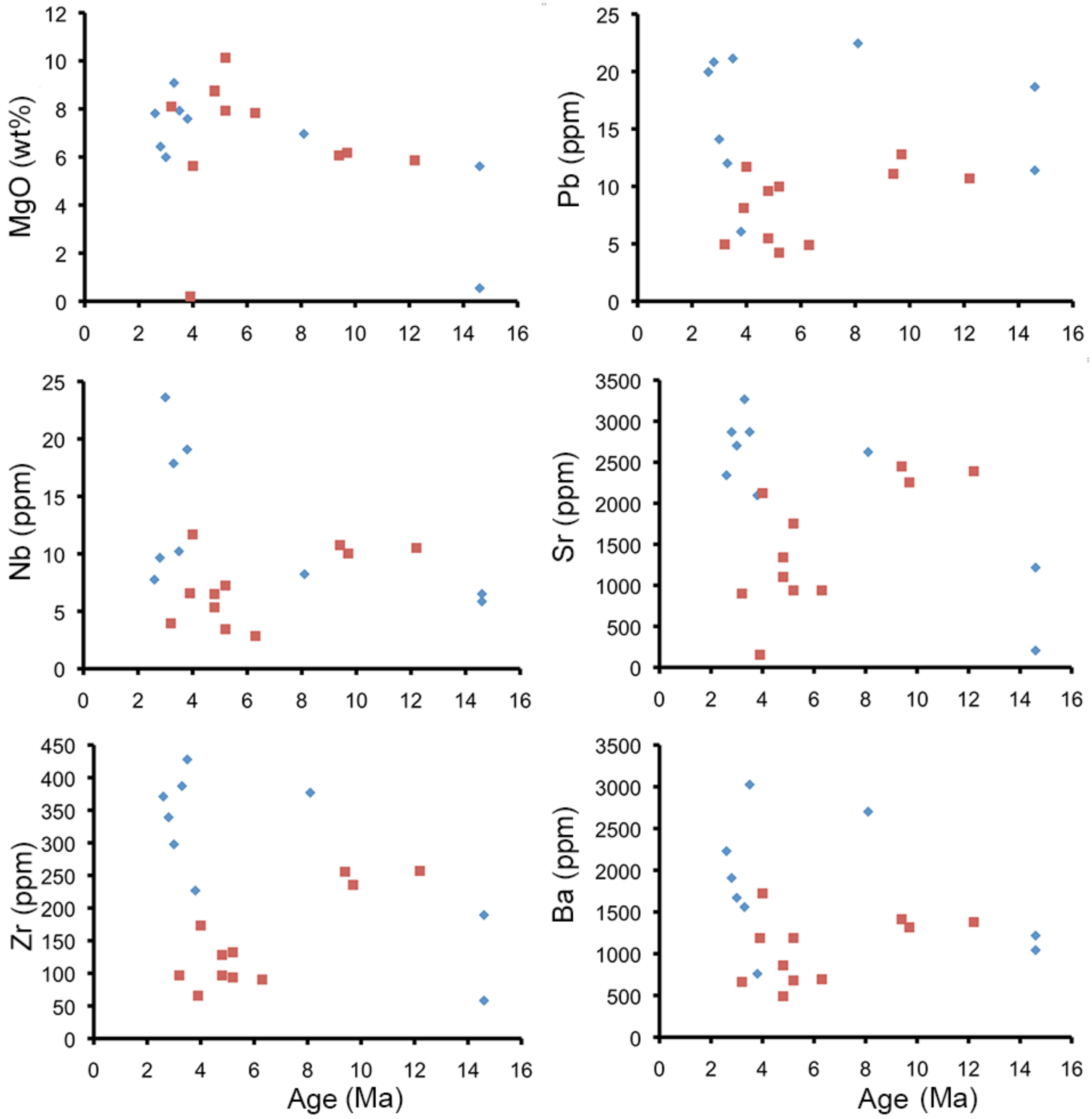

Figure 12: Plots of age (Ma) versus MgO (wt%) and select trace elements (ppm) for bajaites from Baja California, Mexico. Symbols as in Figure 2.

The compositional difference between San Borja and Jaraguay bajaites

San Borja bajaites are generally more alkalic as they are more enriched in alkali elements (e.g., K, Na) and many incompatible trace elements (e.g., Zr, Ba) than Jaraguay bajaites (Figs. 2, 3, 5 - 7, 10). An increase in incompatible elements at a given SiO_2 (e.g., vertical variations in Figs. 2, 3 and 7) is generally attributed to changes in the degree of partial melting of the same mantle source (e.g., Gill, 1981; Pearce, 1996; Pearce et al., 1984; Winchester and Floyd, 1977). That is, a smaller degree of partial melt contains more incompatible elements than a higher degree of partial melt derived from the same source (Blatt et al., 2006). The bajaites are temporally and spatially related (Figs.1, 12), and also have generally similar major element compositions and trace element concentration patterns; these similarities indicate that they may indeed share a common, though not necessarily identical source. Thus, can variable degrees of partial melting of a common source explain the compositional difference between the bajaites?

A semi quantitative method of connecting genetically related lava suites by partial melting, as well as verifying fractional crystallization effects on them, is through the use of ‘process identification diagrams’ (Allegre and Minster, 1978; Hoffman et al., 1983). In these diagrams, which are plots of highly/moderately incompatible trace element ratio against the highly incompatible trace element, cogenetic samples that are related through varying degrees of batch partial melting assume a sub vertical and positive trend. On the contrary, samples that are related through fractional crystallization assume a horizontal trend. This method is utilized in Figure 13, using rare earth

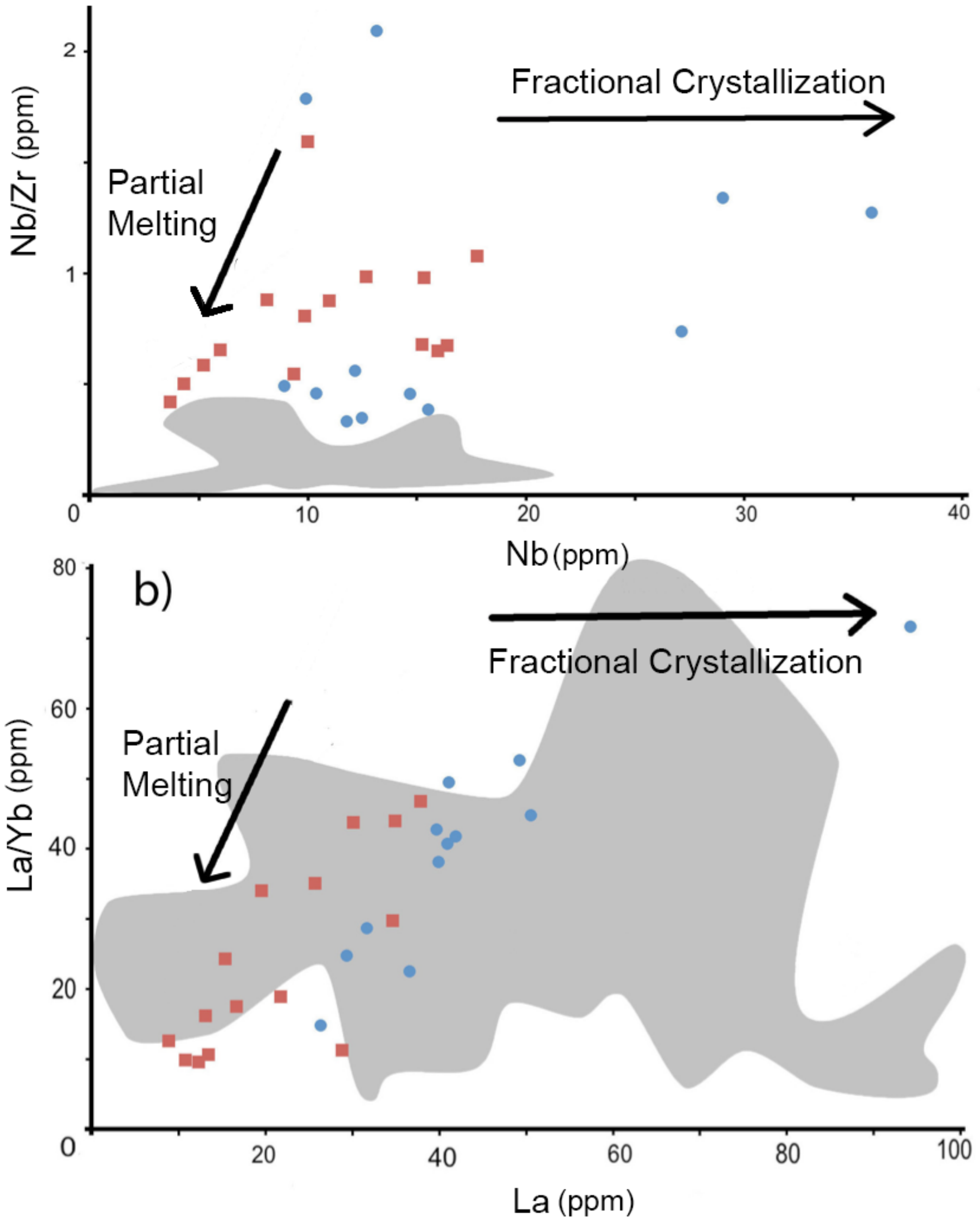

Figure 13: Plot of highly/moderately incompatible trace element ratios against the highly incompatible trace element for representative San Borja and Jaraguay bajaites. Modified after Singer et al. (1996) and Woodhead et al. (1998). Symbols as in Figure 2. The field for global adakites (source literature citations are listed in bibliography), in grey, is shown for reference. Symbols as in Figure 2.

elements La and Yb as well as high field strength elements Nb and Zr. These trace elements were chosen because they are not mobile under hydrothermal conditions and La/Yb and Nb/Zr are mainly fractionated during partial melting of the mantle or during magma mixing (Singer et al., 1996). Data show that although some of the samples, particularly the rhyolites, plot far to the right of the partial melting trend—which is consistent with fractional crystallization from multiple parent magmas—the two bajaite groups do not define any systematic degree of partial melting relationship. Instead, the diagrams as a whole show that San Borja has consistently higher La and Nb content for any given La/Yb and Nb/Zr (or higher degree of fractional crystallization), respectively, than Jaraguay. Hence, the slight though systematic compositional difference between the two bajaite localities is not due to a difference in the degree of partial melting of a common mantle source; but rather, the variation displayed in Figure 13 may systematically be due to fractional crystallization and/or slightly different mantle sources. Another way to constrain the difference between the origin of the two bajaite rock suites is to combine the trace elements Nb, Ti, and Zr with REE (including Y) because these are excellent proxies for subduction zone magmatic processes due to their relatively comparable immobility in subduction zone fluids within the mantle wedge (Pearce, 1996; Pearce et al., 1984). In other words, these elements are highly immobile in the mantle and are conservative during subduction (i.e., they are not transferred to the mantle wedge from the down-going slab). Niobium is more incompatible than Zr and, thus, the behavior of the two elements can be compared and contrasted (Brennan et al., 1993). In Figure 14 their concentrations are expressed as ratios, which are used as analogues for magmatic evolution in a similar way that major oxide concentrations are used (Blatt et al., 2006; Fig. 2). These ratios can be used to confirm that the compositional variation observed in the bajaites is due to magmatic differentiation and/or a direct reflection of the source rather than being due to secondary processes like weathering and metamorphism (Pearce et al., 1984; Pearce and Cann, 1973). In this case, changes in melt composition due to fractional crystallization can be expressed as variations in Zr/TiO_2 compositions, due to the fact that Zr is fractionated much like SiO_2 within magma (Floyd and Winchester, 1975). On the other hand, the degree or depth of partial melting in the mantle source can be represented as changing Nb/Y concentrations because Nb/Y has been shown to be a possible tracer for alkalinity (Pearce and Cann, 1973; Floyd and Winchester, 1975; Wang et al., 2010; Blatt et al., 2006). What this means is a higher Nb/Y ratio would indicate higher alkalinity in the sample, which can suggest a lower degree of partial melt or a greater depth of melting within the source (Blatt et al., 2006). In Figure 14, more alkaline suites plot to the right in the “alkali basalt / trachyandesite / trachyte” fields. Similarly, samples that have undergone fractional crystallization plot toward the top of Figure 11, where the rhyolite and trachyte fields are, respectively.

Figure 14 shows that fractional crystallization can account for a portion of the compositional variation between the two bajaite localities, and the degree or depth of partial melting of the mantle source do not seem to contribute to the variance of the samples. In other words, it can be inferred from Figure 13 that San Borja consistently shows more enrichment than Jaraguay in Zr/TiO_2, indicating that San Borja is more fractionated than Jaraguay. However, beside the couple of San Borja samples that are enriched in the selected trace elements, both bajaite suites generally show wide and

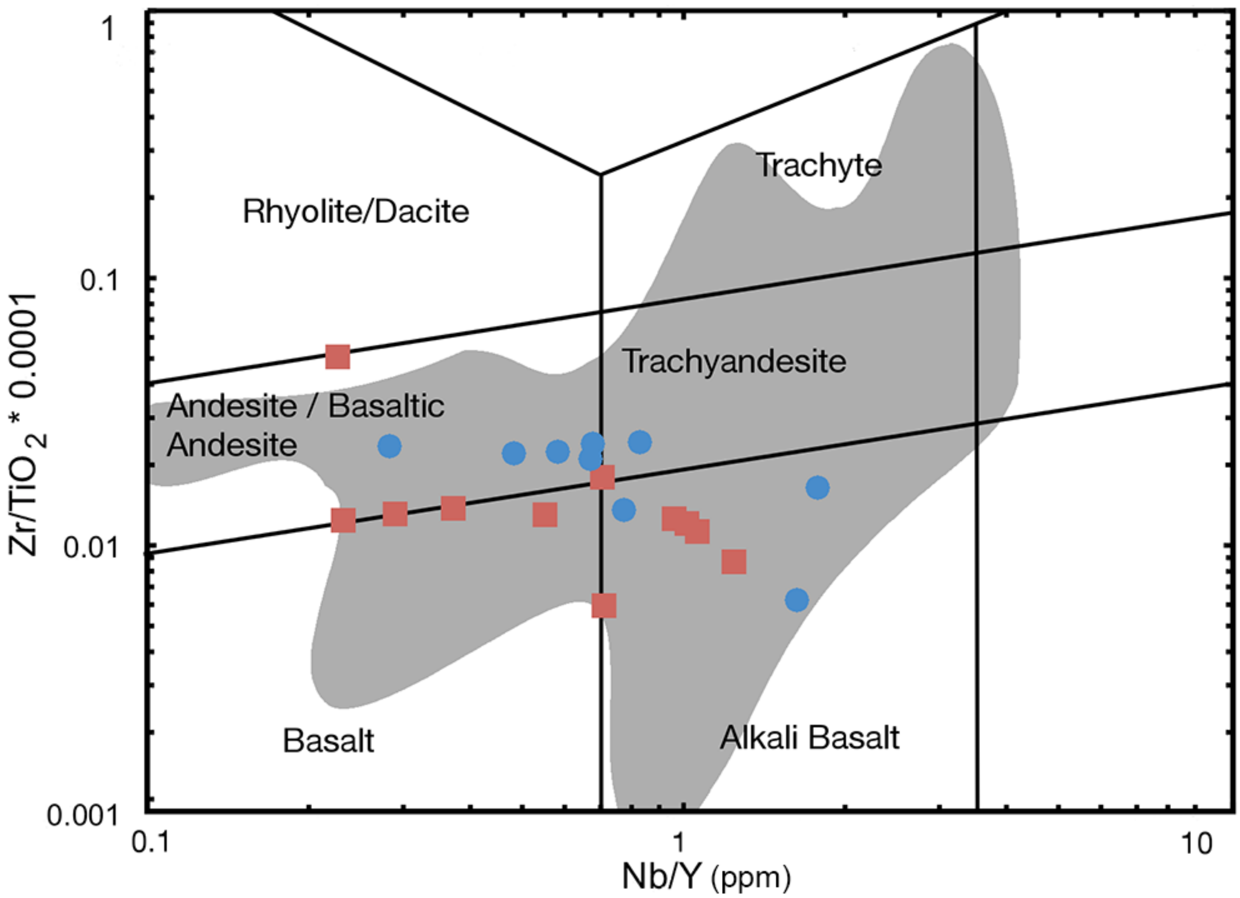

Figure 14: Plot of Zr/TiO$_2$ versuss Nb/Y for representative San Borja and Jaraguay bajaites. Symbols as in Figure 2. Modified after Pearce (1996). More alkaline suites plot to the right in the “alkali basalt/ trachyandesite / trachyte” fields. Similarly, samples that have suffered fractional crystallization plot toward the top, where the rhyolite and trachyte fields are, respectively. The field for global adakites (source literature citations are listed in bibliography), in grey, is shown for reference. Symbols as in Figure 2.

overlapping Nb/Y values; this indicates that they were both produced through a relatively large degree or range of partial melting and/or depths of partial melting. Since the bajaite samples cannot be distinguished in terms of alkalinity, the degree or depth of partial melting of a common source cannot be addressed. However, the trace element variation indicates that a systematic difference in the degree of fractional crystallization may be responsible for the methodical compositional difference between the San Borja and Jaraguay bajaites. Notwithstanding, fractional crystallization cannot explain the variation seen in the isotope ratios of the bajaites, and most certainly cannot explain why we see a variety of Nb/Y ratios.

Although the Jaraguay bajaites have systematically higher $^{143}Nd/^{144}Nd$ and lower $^{87}Sr/^{86}Sr$ than San Borja bajaites (Figure 8), they have overlapping Pb isotopic ratios (Figure 9). Furthermore, the ranges of isotopic values of both rock suites, and all bajaites (or Baja California HMA) in general, are relatively large. This clearly means that although the bajaites may have come from a common mantle source, this source must be compositionally heterogeneous. Consequently, the bulk of the compositional variation of the bajaites originates from the inherent heterogeneity of their common mantle source.

The mantle source of bajaites

It was emphasized earlier that the Jaraguay and San Borja bajaites have some compositional features of global arc lavas, particularly the hallmark depletion in HFSE and enrichment in fluid-mobile elements (Fig. 5). Equally significant is that their Sr and Nd isotopic characteristics, and all bajaites in general, are similar to tose of calc-alkaline arc lavas from Baja California and arc lavas from the TMVB (Figure 8)—an almost east-west rending site of active magmatism that starts sourtheast of the southern tip of Baja California (Verma, 1984, 1989, 1991, 2000, and 2001; Cebria et al., 2011). The Sr and Nd ratios of these Mexican arc lavas also overlap with many other arc lavas, such as from the SVZ in South America (Holm et al., 2014; Lopez-Escobar et al., 1995) and the Setouchi Volcanic Belt in Japan (Shimoda et al., 1998). In terms of $^{206}Pb/^{204}Pb$, the bajaites are again compositionally akin to these arc lavas, except for the Baja calc-alkaline arc lavas (Fig. 9). Significantly, the bajaites are distinctively more radiogenic than the Baja California adakites and calc-alkaline lavas.

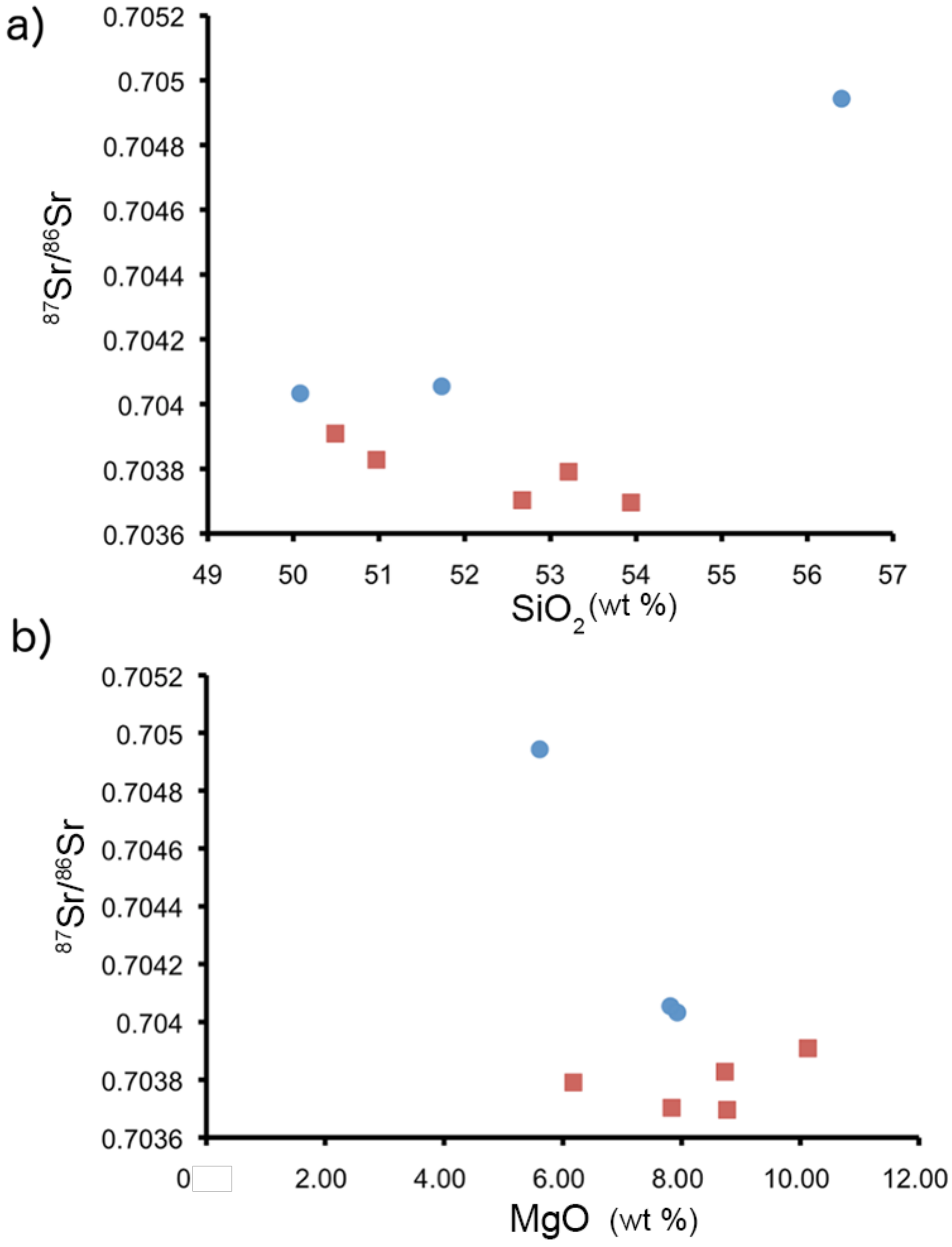

Figure 15: Plots of a) SiO_2 (wt %) versus $^{87}Sr/^{86}Sr$ and b) MgO (wt%) versus $^{87}Sr/^{86}Sr$ for representative bajaites from Baja California, Mexico. Symbols as in figure 2.

Crustal contamination

A possible explanation for the compositional similarity of bajaites with the other arc-related, post subduction lavas in Baja California is through crustal assimilation. That is, crustal rocks may have contaminated bajaites as the magmas transited from their source deep below the crust to the shallow surface. A way to test this process is by plotting $^{87}Sr/^{86}Sr$, which is susceptible to crustal contamination, versus SiO_2 and MgO—two indices for magmatic differentiation (Faure, 2013; Figure 15). A positive correlation between silica and Sr isotopic composition generally indicates crustal contamination. Similarly, an inverse correlation between MgO and $^{87}Sr/^{86}Sr$ would indicate crustal contamination because MgO is higher in basaltic magmas, and decreases as the magma differentiates. However, although samples 12B087C, with 5.61% MgO and 56.40% SiO_2 (Table 1 and Table A1), indeed has the highest $^{87}Sr/^{86}Sr$ at 0.704943 (Table 3), all of the other samples do not show the expected correlation patterns (~50 – 54% SiO_2). In fact, the opposite is true because the Jaraguay bajaites that generally show higher SiO_2 have lower $^{87}Sr/^{86}Sr$ than the volcanics from San Borja. There does not appear to be large enough variation among the MgO versus $^{87}Sr/^{86}Sr$ values for both volcanic fields to establish any correlation. Thus, crustal assimilation or contamination is not responsible for the compositional variation in the bajaites.

The mantle wedge

The bulk of arc lavas are generated through flux-melting of the mantle wedge (e.g. Gill, 1981; Tatsumi et al., 1997; Tatsumi, 2005; Kelemen et al., 2003; Wilson, 1989). The mantle wedge is the portion of the upper mantle located in between the subducting and overriding lithospheric plates, and is typically depleted via multiple episodes of melting in the backarc region (e.g., Pearce, 1996). The mantle wedge subsequently becomes enriched (or metasomatized) due to the addition of fluids that were dehydrated from the downgoing slab. These fluids carry trace elements such as Rb, Pb, and Sr, that are released from the subducting slab through the breakdown of hydrous minerals, such as amphibole, as the slab sinks deeper into the mantle (e.g., You et al., 1996; Wilson, 1989). These fluids lower the solidous of the mantle wedge and, thus, are responsible for generating primary arc magmas. These magmas then fractionate and, most likely, assimilate overlying crustal materials prior to eruption as arc lavas (Gil, 1981; Wilson, 1989).

Since the bajaites are compositionally akin to many arc lavas, and are temporally and spatially related to other post-subduction (~13 to 1 Ma), arc-like lavas (Aguillon-Robles et al., 2001; Benoit et al., 2002; Storey et al., 1989; Rogers et al., 1985; Saunders et al., 1987; Luhr et al., 1995; Calmust et al., 2003; Negrete-Aranda et al., 2014 and 2010; Bellon et al., 2006, Garcia-Amador et al., 2012; Pallares et al., 2007 and 2008), then their source must be a part of the mantle wedge that was formed by prior subduction in the peninsula. Such a source would explain the compositional similarities among bajaites and other post-subduciton, arc related lavas in Baja California, and global arc lavas (e.g., Figs. 5, 8, and 9).

The origin of bajaites

As noted in the Introduction section, knowing more about the petrogenesis of bajaites would lead to a better understanding of continental crust formation (Hofmann, 1988; Rudnick, 2005). Results of this study show that the source of bajaites is the metasomatized mantle wedge and, therefore, is consistent with the link between arc magmatism and modern continental crust formation (Rudnick, 2015; Hofmann, 1988). What needs to be resolved is whether the bajaites were indeed produced through partial melting of the Baja California mantle wedge that was metasomatized simply by slab-derived fluids (see also, Castillo, 2008) or by silicic melts (adakites) produced by partial melting of the subducted basaltic crust (Aguillon-Robles et al., 2002; Pallares et al., 2008; Tatsumi 2006; Rapp et al., 1999).

The $^{87}Sr/^{86}Sr$ and $^{143}Nd/^{144}Nd$ isotope systematics of arc lavas are a highly accurate indicator of slab melting processes (Castillo, 2008). This is because basaltic melts, or adakites, are characteristically enriched in Sr and Nd, which similar to La is a light REE (Gill, 1981; Defant and Drummond, 1993, 1996). The high Sr and Nd contents in a slab melt are due to high-pressure partial melting of subducted oceanic basalt (e.g., Pacific MORB) that has been metamorphosed to eclogite, deep in the subduction zone. This process releases almost all Sr into the resultant melt (or adakite) from the subducted slab, but retains heavy-REE in residual eclogite (Gill, 1981; Defant and Drummond, 1993, 1996; Yogodzinski et al., 1998; Tatsumi, 2006). Significantly, the few adakites in Baja California do contain high Sr and Nd, and are Pacific MORB-like in $^{87}Sr/^{86}Sr$ and $^{143}Nd/^{144}Nd$ (Fig. 8; Aguillon-Robles et al., 2001).

Bajaites have extremely high Sr (up to ~3000ppm; see also, Saunders, 1987; Rogers et al., 1985), which are much higher than typical adakites; they also have high Nd contents (Table 2, Table A2, Fig. 5). Note that, based on the above discussion, the bulk, if not almost all, of these two elements must have come from the subducted

Pacific MORB if the mantle wedge source of bajaites was metasomatized by adakite melt (Aguillon-Robles et al., 2002; Pallares et al., 2007; Tatsumi, 2006). Critically, the $^{87}Sr/^{86}Sr$ and $^{143}Nd/^{144}Nd$ of bajaites do not match Baja California adakites or Pacific MORB (Fig. 8). Instead, the bajaites plot with co-existing calc-alkaline arc lavas in the peninsula, as well as arc lavas from the TMVB. Therefore, the mantle wedge source of bajaites was clearly not metasomatized by slab melt, but rather by slab derived fluids from the downgoing slab beneath Baja California.

Can the Sr and Nd isotopes of bajaites indeed be coming from slab-derived fluids, similar to those in typical arc lavas? The composition of arc lavas is typically modeled as mixtures of DMM and a subduction component that is carried by slab-derived fluids. These fluids typically contain fluid-mobile elements derived primarily from subducted sediments and, to a lesser extent, from the underlying basaltic and lithospheric mantle (e.g. Gil, 1981; Wilson, 1989). To verify if bajaites were produced through the same process, a similar and general modeling approach is adopted below (Figure 16). The mixing curves shown were calculated using a hyperbolic mixing equation as described by Langmuir et al., 1977 (see also Sohn, 2005). The details of calculations and the mixing coefficient “r”, which corresponds to the concentration ratio of end members in the samples, are described in detail in the Appendix section A1. Modeling results show that magma mixing between the depleted mantle (DMM; Workman and Hart, 2005) and fluids derived from average global subducted sediment (GLOSS; Plank and Langmuir, 1977) can produce the observed $^{87}Sr/^{86}Sr$ and $^{143}Nd/^{144}Nd$ ratios of bajaites. Notably, mixing between Pacific MORB melt (adakite) and the mantle wedge—which is typically the upper mantle or DMM—is not an appropriate explanation for the origin of bajaites, as the latter plot outside the DMM—Baja adakites field (Figures 8 and 16; Faure, 2013).

The Pb isotopic ratios of bajaites also argue against the notion that their mantle source was metasomatized by adakite melt (Fig. 9). The bulk of Pb in the mantle wedge must be coming from the subducted slab (Straub and Zellmer, 2012), either by way of direct slab melt or slab derived fluids, because the upper mantle is low in Pb (0.018 ppm; Workman and Hart, 2005). The bajaites contain 4 to 22 ppm Pb, and the majority contain >10 ppm. Thus, if the Pb in bajaites is derived from Pacific MORB melt, then the PB isotopic signature of bajaites should be similar to Baja California adakites, Pacific MORB, or at least plot between the latter and the former. However, the ^{208}Pb/^{204}Pb and ^{206}Pb/^{204}Pb of bajaites are clearly different from those of Pacific MORB or Baja California adakites. Thus, the Pb in bajaites did not come from slab melt. Instead, the bajaites plot between the value of the Pacific MORB (or its depleted upper mantle source) and GLOSS, which supports the conclusion that the mantle wedge source of the bajaites was metasomatized by slab derived fluids.

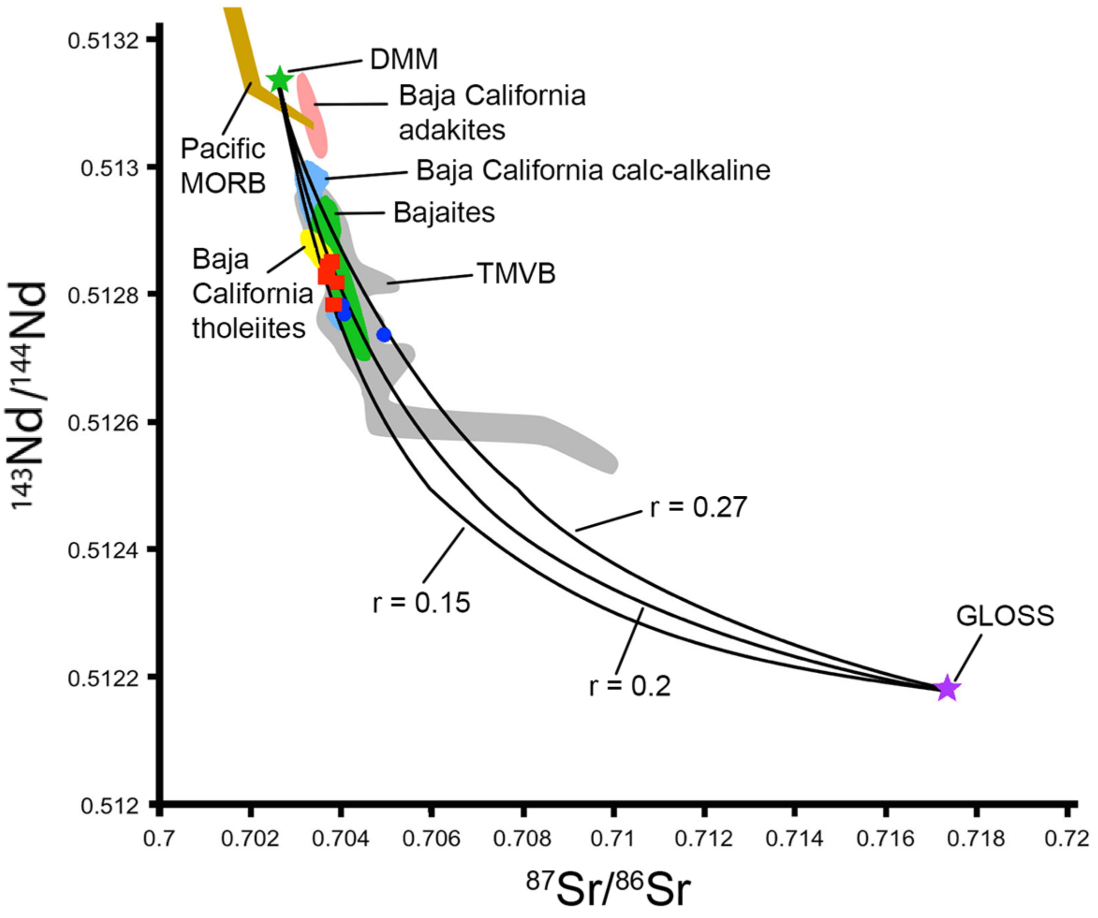

Figure 16: Mixing curves between DMM (green star) and GLOSS (purple star). The grey field represents samples from the TMVB, brown field represents Pacific MORB, pink field represents Baja California adakite, blue field represents Baja California calc-alkaline lavas, yellow field represents Baja California tholeiites, and green field represents Baja California bajaites. Concentration ratio “r” of the curves shown = 0.15, 0.2, and 0.27, respectively, from left to right. Red squares represent Jaraguay samples and blue circles represent San Borja samples. References for these fields are the same as in Figures 7 and 8.

The Th isotopic signature of bajaites also strongly supports the notion that fluids derived from the subducted sediments primarily metasomatized their mantle wedge source (Nauret et al., 2012). The bajaites have very large ^{230}Th excesses (50% to 120%) relative to ^{238}U that were most likely derived from very low degree partial melting of the lithospheric mantle beneath Baja California. Notably, this lithospheric mantle had to be metasomatized by older melts from the residual mantle wedge, which carried a sedimentary component (Nauret et al., 2012).

In addition to isotopic data, some trace element data are suitable indicators of the petrogenetic processes happening below the crust. Specifically, the bajaites are enriched in barium and strontium (Table 2 and Table A2; Figs. 5 and 7), which are fluid-mobile elements (Rudnick, 2005). These enrichments support the idea that a notable amount of subduction-derived fluid must have been present in order to melt the heterogeneous mantle wedge for a prolonged amount of time (i.e. 12 Ma - ~1 Ma; Grove et al., 2012). Additionally, the bajaites are enriched in Zr, which is associated with silicate melt formation (Louvel et al., 2014). This melting may be responsible for post-subduction, arc-related magmatism in Baja California.

Finally, relatively immobile trace elements such as Th, Nd and Yb, combined with the relatively mobile trace elements Sr, can also be used to ascertain whether sediment melting or fluid mobilization is a logical explanation for the trace element signature of these arc volcanic lavas (Woodhead et al., 1998). Specifically, enrichment in Th/Yb in arc lavas has been inferred to be due to a sedimentary component; this can be imparted through melting of sediment (Elliot et al., 1997) or interaction of arc lavas with the overlying crust (Davidson, 1987). On the other hand, enrichment in Sr/Nd is considered to be the result of the input of slab-derived fluids into the mantle wedge (Woodhead et al., 1998). Figure 17 shows that the bajaites, in general, have low Th/Yb, but variable Sr/Nd values. Only a few samples from San Borja display significant Th/Yb enrichment. This means that although there are some degrees of overlap, the sedimentary component in bajaites mostly came from fluids dehydrated from the subducted slab. In detail, however, it is possible that a part of the sedimentary component of the mantle wedge source of San Borja bajaites was, to a limited extent, transported by a small degree of partial melt of the sediment on top of the subducted slab, as well. Overall, figure 17 sheds light on possible sources of bajaites, but does not distinguish them from samples labelled as “adakite” in the literature.

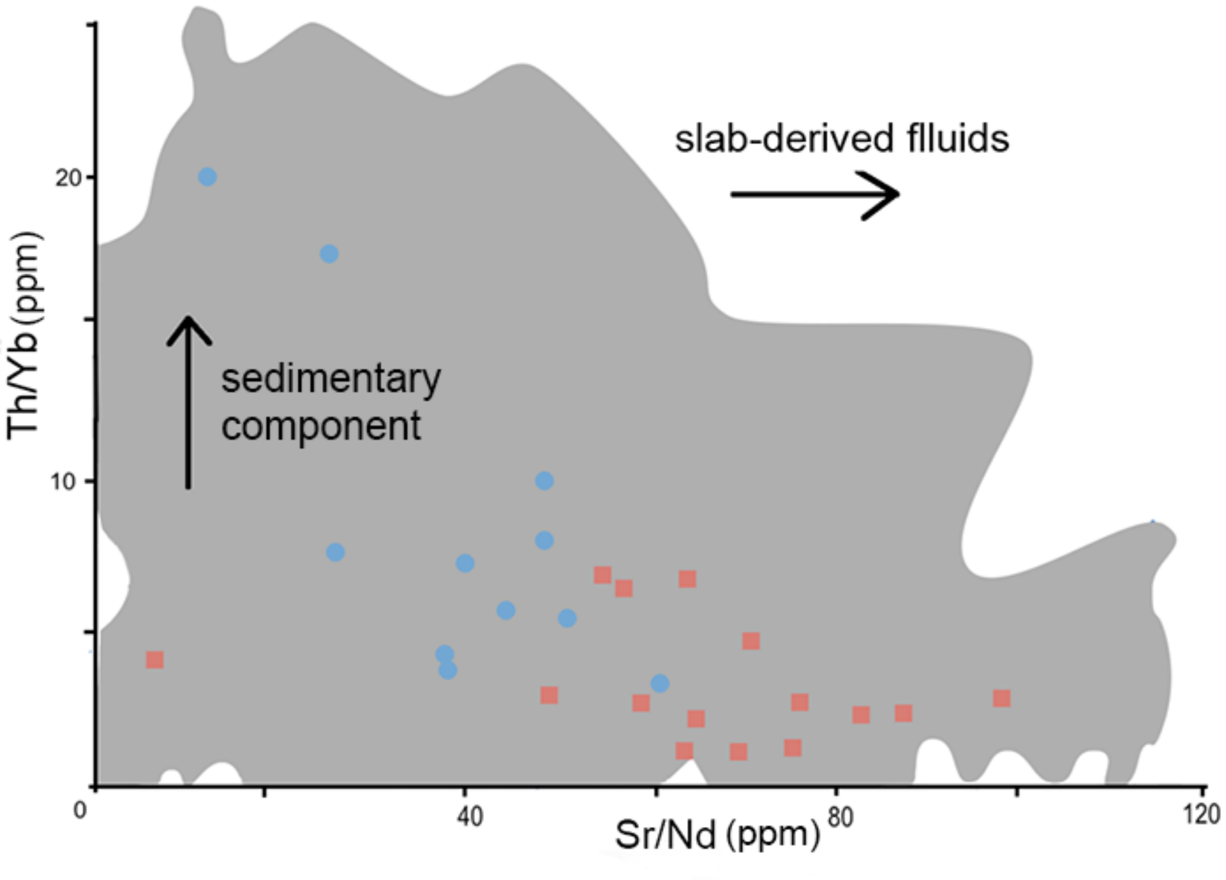

Figure 17: Plot of Th/Yb vs Sr/Nd ratios for bajaites from Baja California. Symbols as in figure 2. Modified after Woodhead (1998). The field for global adakites (source literature citations are listed in bibliography), in grey, is shown for reference. Symbols as in Figure 2.

Summary and Conclusions

Major, trace, and Sr-Nd-Pb isotopic data show that the most probable origin of bajaites from San Borja and Jaraguay volcanic fields in Baja California, Mexico is the result of partial melting of the previously depleted mantle wedge that had been metasomatized by a slab component beneath the peninsula. Direct slab melt—known as adakites—did not play a major role in the production of bajaites. Whole rock geochemistry shows that the bajaites are comparable to other arc lavas that were also derived from the mantle wedge. The Sr, Nd and Pb isotopic values of bajaites are distinct from those of subducted Pacific MORB, or its partial melt, the Baja California adakite. The bajaites were also not produced by mixing of adakite melt and the depleted mantle wedge. On the other hand, the Sr-Nd-Pb isotopic compositions of bajaites can be explained simply through binary mixing between global ocean sediments (GLOSS), representing the subduction component, and the depleted upper mantle source of MORB (DMM), representing the mantle wedge. The other post-subduction lavas in Baja California, Mexico—like niobium enriched basalts, rare alkali lavas, and tholeiites—were most likely produced from the same mantle wedge. Although there are adakites in the Santa Clara volcanic field in Baja California, this study shows that the occurrence of adakites in Baja California may be a local phenomenon that did not have a regional imprint on the rocks from the rest of the peninsula.

Future

More detailed field and lab work is needed in order to better constrain the petrogenetic history of bajaites lavas of Baja California. Specifically, more samples need to be taken in order to complete the basalt to rhyolite sequence in Jaraguay and San Borja volcanic fields, and also to achieve a higher resolution database of the bajaites from Baja California. Additional studies on melt inclusions and phenocrysts will better constrain the petrogenetic end-members and processes that can provide additional evidence and clues on the origin of bajaites. Detailed fieldwork would be very valuable, with emphasis on locating mantle xenoliths and old volcanic vents. Future researchers should gather more samples from surrounding areas, such as the abandoned fossil ridge, to better constrain the isotopic signature of MORB in that area. A geochemical investigation of the ophiolite on the Vizcaino peninsula may also provide important information about the evolution of Baja California.

Appendix

Table A1: Duplicate major element data for bajaites from Baja California, Mexico.

Sample	12B007A	12B007A-LD
Location	San Borja	San Borja
SiO_2	51.08	51.07
TiO_2	1.69	1.69
Al_2O_3	13.52	13.56
FeO*	6.39	6.29
MnO	0.09	0.09
MgO	7.62	7.63
CaO	8.93	8.91
Na_2O	2.80	2.80
K_2O	3.60	3.60
P_2O_5	0.42	0.42
Sum	96.14	96.07

Table A2: Duplicate trace element data for bajaites from Baja California, Mexico

		Li	Sc	Ti	V	Cr	Co	Ni	Cu	Zn	Ga	Ge
12B007A	San Borja	8.4	27.4	11881.7	219.7	329.6	36.6	250.7	69.0	126.7	22.6	1.8
12B007A*	San Borja	6.2	18.7	8967.3	169.8	260.9	28.4	194.3	52.8	106.0	17.2	1.4
12B018B	San Borja	8.8	26.7	10267.0	199.7	323.0	37.5	230.2	61.8	110.6	21.2	2.0
12B018B*	San Borja	9.0	22.7	10162.2	199.1	330.0	38.4	239.4	65.9	142.8	21.1	2.0
12B023B	San Borja	7.1	22.2	9351.0	167.0	238.2	32.0	221.2	59.0	108.1	19.5	1.7
12B023B*	San Borja	7.5	21.4	9868.4	172.7	279.4	32.6	224.7	59.0	102.9	20.1	1.7
12B033B	San Borja	7.4	16.6	17085.9	247.9	293.9	30.8	183.1	32.5	136.5	19.1	1.7
12B033B*	San Borja	10.8	22.2	24837.8	360.3	454.0	44.6	268.0	48.2	195.5	27.8	2.7
12B039C	San Borja	6.8	26.5	8682.9	144.0	336.3	36.9	248.1	49.9	108.4	18.3	1.8
12B039C*	San Borja	6.9	27.5	8840.0	150.3	373.6	37.2	245.4	51.9	105.3	18.0	1.7
12B051A	San Borja	7.7	20.0	7703.5	169.5	328.0	31.6	223.5	53.4	101.7	19.7	1.6
12B051A*	San Borja	7.8	22.4	7932.2	174.7	342.2	33.3	249.1	58.1	140.7	19.9	1.5
12B057B	San Borja	11.6	24.6	16129.7	208.8	301.0	34.5	231.5	61.0	181.6	24.2	2.8
12B057B*	San Borja	11.8	18.1	16428.2	210.7	317.6	35.5	237.6	63.1	173.2	24.8	3.1
12B062B	San Borja	9.5	19.2	10830.5	183.7	350.7	34.9	245.3	61.3	120.4	22.2	1.9
12B062B*	San Borja	9.2	22.5	10657.1	178.6	331.3	33.8	242.4	59.4	124.5	21.8	1.8
12B080C	San Borja	27.1	5.7	1216.2	23.1	8.2	3.8	6.8	8.8	58.0	14.2	0.7
12B080C*	San Borja	26.9	5.8	1392.3	23.9	8.7	3.9	7.4	9.4	65.5	14.4	0.8
12B087C	San Borja	14.3	27.8	6046.4	186.6	252.9	31.4	144.3	40.8	121.4	25.5	1.5
12B087C*	San Borja	11.1	19.8	4632.2	147.2	194.9	24.7	113.3	33.4	95.8	20.5	1.2
12B094D	San Borja	12.8	16.3	6009.2	115.1	281.9	25.5	195.5	26.4	116.2	21.0	1.4
12B094D*	San Borja	12.8	14.8	6115.7	118.7	292.8	25.4	199.6	26.6	93.9	21.4	1.4
12B145B	Jaraguay	8.8	15.5	4063.2	89.2	281.6	29.8	279.2	52.1	102.4	18.0	0.9
12B145B*	Jaraguay	7.3	12.9	3498.7	77.6	244.0	26.0	238.5	46.8	97.0	15.1	0.9
12B172B	Jaraguay	8.3	24.2	3721.0	170.1	259.0	31.4	144.9	52.9	77.1	17.1	1.1
12B172B*	Jaraguay	8.0	24.2	3623.9	166.0	259.2	31.5	150.2	52.4	90.8	16.9	1.1
12B207A	Jaraguay	11.4	24.8	16161.5	299.2	215.2	36.0	114.0	36.4	162.0	25.9	1.8
12B207A*	Jaraguay	7.3	15.1	10529.3	193.1	137.4	23.2	72.6	22.9	98.4	16.7	1.1
12B226C	Jaraguay	12.6	22.4	6126.5	174.9	328.1	38.6	301.9	62.6	124.8	19.9	1.5
12B226C*	Jaraguay	11.4	18.5	5592.4	160.5	304.8	35.6	287.8	56.4	105.5	18.0	1.4

* Lab replicate

Table A2: Duplicate trace element data for bajaites from Baja California, Mexico (continued).

	Rb	Sr	Y	Zr	Nb	Cs	Ba	La	Ce	Pr	Nd	Sm
12B007A	44.6	2868.9	12.3	427.8	10.2	0.3	3025.8	41.8	97.8	13.1	52.6	8
12B007A*	33.7	2170.3	9.3	324.4	7.8	0.3	2256.9	31.5	73.6	10.0	39.1	6
12B018B	30.0	2624.3	17.1	376.9	8.2	0.3	2701.8	50.6	117.4	16.4	66.4	10.7
12B018B*	29.4	2564.8	16.6	382.4	8.3	0.3	2695.5	50.4	117.3	15.8	64.6	10.1
12B023B	34.2	2341.7	11.4	371.0	7.8	0.3	2228.6	39.7	93.5	12.2	48.3	7.6
12B023B*	34.8	2397.3	11.7	379.9	8.1	0.3	2287.3	40.4	94.4	12.6	50.1	7.5
12B033B	11.5	2095.9	11.7	226.8	19.1	0.1	759.9	41.2	101.6	13.9	55.8	8.6
12B033B*	16.7	3021.9	16.9	330.2	27.7	0.1	1085.2	59.6	146.2	20.1	80.0	12.3
12B039C	21.5	2867.9	16.6	339.2	9.7	0.2	1907.3	36.6	90.2	12.0	47.1	7.3
12B039C*	21.4	2848.7	16.8	352.0	9.7	0.2	1885.4	36.6	90.6	12.0	48.2	7.3
12B051A	19.0	2527.5	13.2	236.6	6.8	0.2	1442.0	41.3	94.3	12.5	49.8	8.1
12B051A*	19.3	2587.5	13.4	242.0	6.9	0.2	1445.2	41.3	94.9	12.6	50.5	7.9
12B057B	18.2	3266.6	23.0	387.0	17.9	0.2	1559.3	94.3	231.2	31.6	126.5	20.4
12B057B*	18.1	3247.6	23.0	387.7	18.2	0.2	1558.5	94.3	230.7	31.6	126.9	20.2
12B062B	14.8	2702.4	13.3	297.7	23.6	0.2	1669.9	49.2	115.7	15.4	61.2	9.8
12B062B*	14.3	2678.8	13.5	294.9	23.2	0.2	1673.2	48.6	115.7	15.6	61.0	9.3
12B080C	167.2	206.0	9.6	58.1	6.5	5.6	1216.7	31.7	56.3	5.6	17.0	2.5
12B080C*	167.2	206.1	9.7	59.7	7.4	5.7	1214.0	31.9	57.4	5.6	17.3	2.5
12B087C	44.3	1216.6	20.6	189.4	5.9	2.1	1042.6	26.4	58.4	7.8	32.2	6.4
12B087C*	34.9	966.9	16.3	150.1	4.6	1.6	832.2	20.9	46.4	6.2	25.5	5.1
12B094D	24.5	1760.9	12.2	229.1	8.0	0.3	1432.8	39.9	84.6	9.9	36.4	5.6
12B094D*	25.0	1787.1	12.5	231.8	8.2	0.3	1478.5	40.5	85.5	10.0	36.7	5.7
12B145B	10.4	1341.0	9.2	128.1	6.5	0.2	860.1	16.6	35.6	4.2	16.3	2.9
12B145B*	8.5	1101.5	7.7	106.8	5.7	0.2	702.3	13.5	29.4	3.4	13.3	2.4
12B172B	9.0	938.6	12.3	90.4	2.8	0.1	694.2	13.4	28.7	3.6	14.8	2.8
12B172B*	9.0	937.5	12.5	89.8	2.9	0.1	694.8	13.4	28.9	3.7	14.9	2.7
12B207A	10.0	1843.9	15.3	163.9	10.1	0.3	975.6	21.7	51.1	6.9	28.6	5.5
12B207A*	6.4	1193.2	9.7	106.0	6.5	0.2	653.2	14.1	33.0	4.6	18.6	3.4
12B226C	7.8	1752.6	13.1	132.2	7.2	0.1	1187.9	34.6	75.5	9.5	35.8	5.7
12B226C*	7.0	1566.9	11.6	119.0	6.5	0.1	1064.5	30.7	67.7	8.5	32.2	5.1

* Lab replicate

Table A2: Duplicate trace element data for bajaites from Baja California, Mexico (continued).

	Eu	Gd	Tb	Dy	Ho	Er	Tm	Yb	Lu	Hf	Ta	Pb	Th	U
12B007A	3.0	6.5	0.6	2.6	0.5	1.3	0.1	1.0	0.1	11.0	0.5	21.1	6.9	1.9
12B007A*	2.3	4.7	0.5	1.9	0.4	1.0	0.1	0.7	0.1	8.3	0.4	16.3	5.1	1.5
12B018B	3.4	8.6	0.8	3.4	0.6	1.6	0.2	1.1	0.2	9.9	0.4	22.4	8.2	1.9
12B018B*	3.3	8.1	0.8	3.2	0.5	1.5	0.2	1.1	0.2	9.7	1.8	22.2	7.8	1.8
12B023B	2.7	6.1	0.6	2.5	0.4	1.2	0.1	0.9	0.1	9.2	0.4	20.0	7.4	1.6
12B023B*	2.7	6.1	0.6	2.5	0.4	1.2	0.2	0.9	0.1	9.8	0.4	20.9	7.7	1.6
12B033B	2.4	6.6	0.6	2.7	0.4	1.1	0.1	0.8	0.1	5.3	0.9	6.1	3.5	1.0
12B033B*	3.4	9.8	0.9	3.8	0.6	1.7	0.2	1.2	0.1	7.7	1.3	9.3	5.1	1.5
12B039C	2.6	6.2	0.7	3.3	0.6	1.8	0.3	1.6	0.2	8.7	0.5	20.8	5.5	1.5
12B039C*	2.6	6.2	0.7	3.3	0.6	1.8	0.2	1.6	0.2	8.9	0.5	19.8	5.5	1.5
12B051A	2.4	6.4	0.7	2.8	0.5	1.4	0.2	1.0	0.1	5.6	0.3	14.4	5.5	1.4
12B051A*	2.4	6.3	0.7	2.7	0.5	1.4	0.2	1.1	0.1	5.6	0.3	14.4	5.5	1.4
12B057B	4.8	15.7	1.5	5.8	0.9	2.2	0.2	1.3	0.2	8.9	0.9	12.0	10.0	2.8
12B057B*	5.0	15.8	1.5	5.6	0.9	2.2	0.2	1.3	0.2	8.8	0.9	12.0	9.9	2.7
12B062B	2.8	7.6	0.7	3.0	0.5	1.3	0.2	0.9	0.1	7.6	1.4	14.1	5.4	1.3
12B062B*	2.8	7.8	0.7	3.1	0.5	1.4	0.2	0.9	0.1	7.4	1.4	14.1	5.3	1.3
12B080C	0.8	2.6	0.3	1.6	0.3	1.0	0.2	1.1	0.2	2.1	0.7	18.7	22.1	4.1
12B080C*	0.8	2.7	0.3	1.5	0.3	1.0	0.2	1.1	0.2	2.2	0.8	18.4	22.0	4.2
12B087C	2.1	6.0	0.8	4.0	0.8	2.0	0.3	1.8	0.3	5.2	0.3	11.4	6.9	2.1
12B087C*	1.7	4.7	0.6	3.1	0.6	1.6	0.2	1.5	0.2	3.8	0.3	9.4	5.5	1.6
12B094D	1.9	5.0	0.5	2.4	0.4	1.2	0.2	1.0	0.1	5.4	0.4	14.0	10.4	1.8
12B094D*	1.9	5.1	0.6	2.5	0.5	1.3	0.2	1.0	0.2	5.5	0.5	14.4	10.7	1.9
12B145B	1.1	2.7	0.3	1.8	0.3	1.0	0.1	0.9	0.1	3.2	0.3	9.6	2.2	0.5
12B145B*	0.9	2.1	0.3	1.5	0.3	0.8	0.1	0.7	0.1	2.7	0.3	7.9	1.8	0.4
12B172B	1.2	2.7	0.4	2.1	0.4	1.3	0.2	1.3	0.2	2.1	0.2	4.9	1.4	0.4
12B172B*	1.2	2.7	0.4	2.2	0.5	1.3	0.2	1.3	0.2	2.2	0.2	5.2	1.5	0.4
12B207A	2.1	4.9	0.6	3.2	0.5	1.5	0.2	1.1	0.2	4.1	0.5	7.7	2.5	0.6
12B207A*	1.4	3.2	0.4	2.1	0.4	1.0	0.1	0.8	0.1	2.6	0.3	5.1	1.6	0.4
12B226C	1.8	5.1	0.5	2.5	0.5	1.3	0.2	1.2	0.2	3.3	0.4	10.0	3.4	0.7
12B226C*	1.6	4.3	0.5	2.3	0.4	1.2	0.2	1.0	0.1	3.1	0.3	8.2	3.0	0.6

---

* Lab replicate

A1. Mixing hyperbola calculation.

Using the hyperbolic mixing equation for magma mixing, as described in Langmuir et al. (1977):

$Ax + Bxy + Cy + D = 0$

$A = a_2b_1y_2 - a_1b_2y_1$

$B = a_1b_2 - a_2b_1$

$C = a_2b_1x_1 = a_1b_2x_2$

$D = a_1b_2x_2y_1 - a_2b_1x_1y_2$

$r = a_1b_2/a_2b_1$

Now, using the substitution a1b2 = ra2b1, as described in Sohn, 2005:

$A'x + B'xy + C'y + D' = 0$

$A' = Y_2 - Y_1r$

$B' = r-1$

$C' = X_1-X_2r$

$D'= Y_1X_2r - Y_2X_1$

where $(X_1,Y_1) = (^{87/86}Sr_{DMM},^{144/143}Nd_{DMM})$, and $(X_2, Y_2) = (^{87/86}Sr_{GLOSS},^{144/143}Nd_{GLOSS})$.

Bibliography

Aguillón-Robles A, Calmus T, Benoit M, Bellon H, Maury RC, Cotten J, Bourgois J, Michaud F. Late Miocene adakites and Nb-enriched basalts from Vizcaino Peninsula, Mexico: Indicators of East Pacific Rise subduction below southern Baja California?. Geology. 2001 Jun 1;29(6):531-4.

Aguillón-Robles A. *Subduction de dorsale et évolution du magmatisme associé: exemple de la Basse Californie (Mexique) du Miocène au Quaternaire* (Doctoral dissertation, Brest).

Aitchison JC, Ali JR, Chan A, Davis AM, Lo CH. Tectonic implications of felsic tuffs within the Lower Miocene Gangrinboche conglomerates, southern Tibet. Journal of Asian Earth Sciences. 2009 Mar 31;34(3):287-97.

Allegre CJ, Minster JF. Quantitative models of trace element behavior in magmatic processes. Earth and Planetary Science Letters. 1978 Feb 1;38(1):1-25.

Andrews BJ, Gardner JE, Housh TB. Repeated recharge, assimilation, and hybridization in magmas erupted from El Chichón as recorded by plagioclase and amphibole phenocrysts. Journal of Volcanology and Geothermal Research. 2008 Aug 20;175(4):415-26.

Atwater T. Implications of plate tectonics for the Cenozoic tectonic evolution of western North America. Geological Society of America Bulletin. 1970 Dec 1;81(12):3513-36.

Atwater T. Plate tectonic history of the northeast Pacific and western North America. The eastern Pacific Ocean and Hawaii: Boulder, Colorado, Geological Society of America, Geology of North America, v. N. 1989:21-72.

Barajas SM, de Miguel Beascoechea E. Exposición Nacional de ovino y caprino. Agricultura: Revista agropecuaria. 1986(646):358-9.

Beate B, Monzier M, Spikings R, Cotten J, Silva J, Bourdon E, Eissen JP. Mio–Pliocene adakite generation related to flat subduction in southern Ecuador: the Quimsacocha volcanic center. Earth and Planetary Science Letters. 2001 Nov 15;192(4):561-70.

Bebout GE. Metasomatism in subduction zones of subducted oceanic slabs, mantle wedges, and the slab-mantle interface. InMetasomatism and the Chemical Transformation of Rock 2013 (pp. 289-349). Springer, Berlin, Heidelberg.

Bellon H, Aguillón-Robles A, Calmus T, Maury RC, Bourgois J, Cotten J. La Purísima volcanic field, Baja California Sur (Mexico): Miocene to Quaternary volcanism related to subduction and opening of an asthenospheric window. Journal of Volcanology and Geothermal Research. 2006 Apr 15;152(3):253-72.

Benoit M, Aguillon-Robles A, Calmus T, Maury RC, Bellon H, Cotten J, Bourgois J, Michaud F. Geochemical diversity of Late Miocene volcanism in southern Baja California, Mexico: implication of mantle and crustal sources during the opening of an asthenospheric window. The Journal of Geology. 2002 Nov;110(6):627-48.

Blatt H, Tracy R, Owens B. Petrology: igneous, sedimentary, and metamorphic. Macmillan; 2006.

Bonini JA, Baldwin SL. Mesozoic metamorphic and middle to late Tertiary magmatic events on Magdalena and Santa Margarita Islands, Baja California Sur, Mexico: Implications for the tectonic evolution of the Baja California continental borderland. Geological Society of America Bulletin. 1998 Aug 1;110(8):1094-104.

Bourdon E, Eissen JP, Monzier M, Robin C, Martin H, Cotten J, Hall ML. Adakite-like lavas from Antisana Volcano (Ecuador): evidence for slab melt metasomatism beneath Andean Northern Volcanic Zone. Journal of Petrology. 2002 Feb 1;43(2):199-217.

Bowen NL. The reaction principle in petrogenesis. The Journal of Geology. 1922 Apr 1;30(3):177-98.

Breitsprecher K, Thorkelson DJ, Groome WG, Dostal J. Geochemical confirmation of the Kula-Farallon slab window beneath the Pacific Northwest in Eocene time. Geology. 2003 Apr 1;31(4):351-4.

Brenan JM, Shaw HF, Phinney DL, Ryerson FJ. Rutile-aqueous fluid partitioning of Nb, Ta, Hf, Zr, U and Th: implications for high field strength element depletions in island-arc basalts. Earth and Planetary Science Letters. 1994 Dec 1;128(3-4):327-39.

Busby C, Smith D, Morris W, Fackler-Adams B. Evolutionary model for convergent margins facing large ocean basins: Mesozoic Baja California, Mexico. Geology. 1998 Mar 1;26(3):227-30.

Busby C. Continental growth at convergent margins facing large ocean basins: a case study from Mesozoic convergent-margin basins of Baja California, Mexico. Tectonophysics. 2004 Nov 8;392(1-4):241-77.

Cawood PA, Kroner A, Pisarevsky S. Precambrian plate tectonics: criteria and evidence. GSA today. 2006 Jul;16(7):4.

Calmus T, Aguillón-Robles A, Maury RC, Bellon H, Benoit M, Cotten J, Bourgois J, Michaud F. Spatial and temporal evolution of basalts and magnesian andesites (“bajaites”) from Baja California, Mexico: the role of slab melts. Lithos. 2003 Jan 31;66(1):77-105.

Calmus T, Pallares C, Maury RC, Aguillón-Robles A, Bellon H, Benoit M, Michaud F. Volcanic markers of the post-subduction evolution of Baja California and Sonora, Mexico: Slab tearing versus lithospheric rupture of the Gulf of California. Pure and Applied Geophysics. 2011 Aug 1;168(8-9):1303-30.

Carmichael IS. The andesite aqueduct: perspectives on the evolution of intermediate magmatism in west-central (105–99 W) Mexico. Contributions to Mineralogy and Petrology. 2002 Sep 1;143(6):641-63.

Castillo PR, Klein E, Bender J, Langmuir C, Shirey S, Batiza R, White W. Petrology and Sr, Nd, and Pb isotope geochemistry of mid-ocean ridge basalt glasses from the 11 45′ N to 15 00′ N segment of the East Pacific Rise. Geochemistry, Geophysics, Geosystems. 2000 Nov;1(11).

Castillo PR, Rigby SJ, Solidum RU. Origin of high field strength element enrichment in volcanic arcs: Geochemical evidence from the Sulu Arc, southern Philippines. Lithos. 2007 Sep 30;97(3):271-88.

Castillo PR. Origin of the adakite–high-Nb basalt association and its implications for postsubduction magmatism in Baja California, Mexico. Geological Society of America Bulletin. 2008 Mar 1;120(3-4):451-62.

Castillo PR. Adakite petrogenesis. Lithos. 2012 Mar 1;134:304-16.

Castillo PR, Hilton DR, Halldórsson SA. Trace element and Sr-Nd-Pb isotope geochemistry of Rungwe Volcanic Province, Tanzania: Implications for a superplume source for East Africa Rift magmatism. Frontiers in Earth Science. 2014 Sep 8;2:21.

Castillo PR. The recycling of marine carbonates and sources of HIMU and FOZO ocean island basalts. Lithos. 2015 Feb 1;216:254-63.

Cebriá JM, Martiny BM, López-Ruiz J, Morán-Zenteno DJ. The Parícutin calc-alkaline lavas: New geochemical and petrogenetic modelling constraints on the crustal assimilation process. Journal of Volcanology and Geothermal Research. 2011 Apr 15;201(1):113-25.

Chashchin AA, Nechaev VP, Nechaeva EV, Blokhin MG. Discovery of Eocene adakites in Primor’e. InDoklady Earth Sciences 2011 Jun 1 (Vol. 438, No. 2, pp. 744-749). SP MAIK Nauka/Interperiodica.

Chiaradia M. Adakite-like magmas from fractional crystallization and melting-assimilation of mafic lower crust (Eocene Macuchi arc, Western Cordillera, Ecuador). Chemical Geology. 2009 Jul 30;265(3):468-87.

Chung SL, Liu D, Ji J, Chu MF, Lee HY, Wen DJ, Lo CH, Lee TY, Qian Q, Zhang Q. Adakites from continental collision zones: melting of thickened lower crust beneath southern Tibet. Geology. 2003 Nov 1;31(11):1021-4.

Conly AG, Brenan JM, Bellon H, Scott SD. Arc to rift transitional volcanism in the Santa Rosalia region, Baja California Sur, Mexico. Journal of Volcanology and Geothermal Research. 2005 Apr 15;142(3):303-41.

Danyushevsky LV, Falloon TJ, Crawford AJ, Tetroeva SA, Leslie RL, Verbeeten A. High-Mg adakites from Kadavu Island Group, Fiji, southwest Pacific: Evidence for the mantle origin of adakite parental melts. Geology. 2008 Jun 1;36(6):499-502.

Davidson JP. Crustal contamination versus subduction zone enrichment: examples from the Lesser Antilles and implications for mantle source compositions of island arc volcanic rocks. Geochimica et Cosmochimica Acta. 1987 Aug 1;51(8):2185-98.

Day JM, Peters BJ, Janney PE. Oxygen isotope systematics of South African olivine melilitites and implications for HIMU mantle reservoirs. Lithos. 2014 Aug 31;202:76-84.

De Astis G, Peccerillo A, Kempton PD, La Volpe L, Wu TW. Transition from calc-alkaline to potassium-rich magmatism in subduction environments: geochemical and Sr, Nd, Pb isotopic constraints from the island of Vulcano (Aeolian arc). Contributions to Mineralogy and Petrology. 2000 Oct 1;139(6):684-703.

Defant MJ, Drummond MS. Derivation of some modern arc magmas by melting of young subducted lithosphere. nature. 1990 Oct;347(6294):662.

Defant MJ, Drummond MS. Mount St. Helens: potential example of the partial melting of the subducted lithosphere in a volcanic arc. Geology. 1993 Jun 1;21(6):547-50.

Dhuime B, Hawkesworth CJ, Cawood PA, Storey CD. A change in the geodynamics of continental growth 3 billion years ago. Science. 2012 Mar 16;335(6074):1334-6.

Drummond MS, Defant MJ, Kepezhinskas PK. Petrogenesis of slab-derived trondhjemite–tonalite–dacite/adakite magmas. Earth and Environmental Science Transactions of the Royal Society of Edinburgh. 1996;87(1-2):205-15.

Eakins BW, Lonsdale PF, Fletcher JM, Ledesma JV. Geomorphology of the Southern Gulf of California Seafloor. InAGU Fall Meeting Abstracts 2004 Dec.

Elliott T, Plank T, Zindler A, White W, Bourdon B. Element transport from slab to volcanic front at the Mariana arc. Journal of Geophysical Research: Solid Earth. 1997 Jul 10;102(B7):14991-5019.

Falloon TJ, Danyushevsky LV, Crawford AJ, Meffre S, Woodhead JD, Bloomer SH. Boninites and adakites from the northern termination of the Tonga Trench: implications for adakite petrogenesis. Journal of Petrology. 2008 Jan 4;49(4):697-715.

Faure, G Principles of Isotope Geology. Wiley, Santa Barbara, CA. 1977.

Faure G. Origin of igneous rocks: the isotopic evidence. Springer Science & Business Media; 2013 Mar 9.

Feigenson MD, Hofmann AW, Spera FJ. Case studies on the origin of basalt. Contributions to mineralogy and petrology. 1983 Dec 1;84(4):390-405.

Floyd PA, Winchester JA. Magma type and tectonic setting discrimination using immobile elements. Earth and Planetary science letters. 1975 Sep 1;27(2):211-8.

Foley FV, Pearson NJ, Rushmer T, Turner S, Adam J. Magmatic evolution and magma mixing of Quaternary adakites at Solander and little Solander Islands, New Zealand. Journal of Petrology. 2012 Dec 5;54(4):703-44.

Fujinawa A, Green TH. Partitioning behaviour of Hf and Zr between amphibole, clinopyroxene, garnet and silicate melts at high pressure. European Journal of Mineralogy. 1997 Jun 26:379-92.

Gao S, Rudnick RL, Yuan HL, Liu XM, Liu YS, Xu WL, Ling WL, Ayers J, Wang XC, Wang QH. Recycling lower continental crust in the North China craton. Nature. 2004 Dec;432(7019):892.

Gao XF, Feng G, Fan WM, Li CW, Li XY. Origin of late Mesozoic intermediate-felsic volcanic rocks from the northern Da Hinggan Mountain, NE China. Acta Petrologica Sinica. 2005 May 1;21(3):737-48.

Gao Y, Hou Z, Kamber BS, Wei R, Meng X, Zhao R. Adakite-like porphyries from the southern Tibetan continental collision zones: evidence for slab melt metasomatism. Contributions to Mineralogy and Petrology. 2007 Jan 1;153(1):105-20.

Garcia-Amador BI, Alva-Valdivia LM, Canon-Tapia E. Paleomagnetic study of the monogenetic volcanism in San Borja and Jaraguay, Baja California Norte, Mexico. InAGU Fall Meeting Abstracts 2012 Dec.

Gastil G, Morgan GJ, Krummenacher D. Mesozoic history of peninsular California and related areas east of the Gulf of California.

Gazel E, Hoernle K, Carr MJ, Herzberg C, Saginor I, Van den Bogaard P, Hauff F, Feigenson M, Swisher C. Plume–subduction interaction in southern Central America: Mantle upwelling and slab melting. Lithos. 2011 Jan 31;121(1):117-34.

Gill JB. Orogenic andesites and plate tectonics. Springer Science & Business Media; 2012 Dec 6.

Govindaraju K. 1994 compilation of working values and sample description for 383 geostandards. Geostandards newsletter. 1994 Jul;18:1-58.

Grove TL, Till CB, Krawczynski MJ. The role of H2O in subduction zone magmatism. Annual Review of Earth and Planetary Sciences. 2012 May 30;40:413-39.

Guo F, Fan W, Li C. Geochemistry of late Mesozoic adakites from the Sulu belt, eastern China: magma genesis and implications for crustal recycling beneath continental collisional orogens. Geological Magazine. 2006 Jan;143(1):1-3.

Guo F, Nakamuru E, Fan W, Kobayoshi K, Li C. Generation of Palaeocene adakitic andesites by magma mixing; Yanji Area, NE China. Journal of Petrology. 2007 Feb 2;48(4):661-92.

Hausback, B. P. Cenozoic volcanic and tectonic evolution of Baja California Sur, Mexico. (1984): 219-236.

Harker A. The natural history of igneous rocks. Cambridge University Press; 2011 May 19.

Hidalgo PJ, Vogel TA, Rooney TO, Currier RM, Layer PW. Origin of silicic volcanism in the Panamanian arc: evidence for a two-stage fractionation process at El Valle volcano. Contributions to Mineralogy and Petrology. 2011 Dec 1;162(6):1115-38.

Hildreth W. Gradients in silicic magma chambers: implications for lithospheric magmatism. Journal of Geophysical Research: solid earth. 1981 Nov 10;86(B11):10153-92.

Hofmann AW. Chemical differentiation of the Earth: the relationship between mantle, continental crust, and oceanic crust. Earth and Planetary Science Letters. 1988 Nov 18;90(3):297-314.

Holm PM, Søager N, Dyhr CT, Nielsen MR. Enrichments of the mantle sources beneath the Southern Volcanic Zone (Andes) by fluids and melts derived from abraded upper continental crust. Contributions to Mineralogy and Petrology. 2014 May 1;167(5):1004.

Hurley PM. Correction to: Absolute abundance and distribution of Rb, K and Sr in the earth. Geochimica et Cosmochimica Acta. 1968 Sep 1;32(9):1025-30.

Imai N, TERASHIMA S, ITOH S, ANDO A. 1994 compilation of analytical data for minor and trace elements in seventeen GSJ geochemical reference samples,“Igneous rock series”. Geostandards Newsletter. 1995 Oct;19(2):135-213.

Ishiwatari A, Yanagida Y, Li YB, Ishii T, Haraguchi S, Koizumi K, Ichiyama Y, Umeka M. Dredge petrology of the boninite-and adakite-bearing Hahajima Seamount of the Ogasawara (Bonin) forearc: An ophiolite or a serpentinite seamount? §. Island Arc. 2006 Mar;15(1):102-18.

Jagoutz O, Kelemen PB. Role of arc processes in the formation of continental crust. Annual Review of Earth and Planetary Sciences. 2015 May 30;43:363-404.

Jiang YH, Jiang SY, Ling HF, Dai BZ. Low-degree melting of a metasomatized lithospheric mantle for the origin of Cenozoic Yulong monzogranite-porphyry, east Tibet: geochemical and Sr–Nd–Pb–Hf isotopic constraints. Earth and Planetary Science Letters. 2006 Jan 31;241(3-4):617-33.

Johnson D, Hooper P, Conrey R. XRF Method XRF Analysis of Rocks and Minerals for Major and Trace Elements on a Single Low Dilution Li-Tetraborate Fused Bead. Adv. X-ray anal. 1999;41:843-67.

Kang ZQ, Xu JF, Chen JL, Wang BD. Geochemistry and origin of Cretaceous adakites in Mamuxia Formation, Sangri Group, South Tibet. Geochimica. 2009;38(4):334-44.

Kang ZQ, Xu JF, Wilde SA, Feng ZH, Chen JL, Wang BD, Fu WC, Pan HB. Geochronology and geochemistry of the Sangri Group Volcanic Rocks, Southern Lhasa Terrane: implications for the early subduction history of the Neo-Tethys and Gangdese Magmatic Arc. Lithos. 2014 Jul 1;200:157-68.

Kay RW, Sun SS, Lee-Hu CN. Pb and Sr isotopes in volcanic rocks from the Aleutian Islands and Pribilof Islands, Alaska. Geochimica et Cosmochimica Acta. 1978 Mar 1;42(3):263-73.

Kay RW. Aleutian magnesian andesites: melts from subducted Pacific Ocean crust. Journal of Volcanology and Geothermal Research. 1978 Aug 1;4(1-2):117-32.

Kay SM, Ramos VA, Marquez M. Evidence in Cerro Pampa volcanic rocks for slab-melting prior to ridge-trench collision in southern South America. The journal of Geology. 1993 Nov 1;101(6):703-14.

Kelemen PB, Shimizu N, Dunn T. Relative depletion of niobium in some arc magmas and the continental crust: partitioning of K, Nb, La and Ce during melt/rock reaction in the upper mantle. Earth and Planetary Science Letters. 1993 Dec 1;120(3-4):111-34.

Kelemen PB. Genesis of high Mg# andesites and the continental crust. Contributions to Mineralogy and Petrology. 1995 May 1;120(1):1-9.

Kelemen PB, Rilling JL, Parmentier EM, Mehl L, Hacker BR. Thermal structure due to solid-state flow in the mantle wedge beneath arcs. Inside the subduction factory. 2004 Jan 1;138:293-311.

Kepezhinskas P, Defant MJ, Drummond MS. Progressive enrichment of island arc mantle by melt-peridotite interaction inferred from Kamchatka xenoliths. Geochimica et Cosmochimica Acta. 1996 Apr 1;60(7):1217-29.

Kimbrough DL, Smith DP, Mahoney JB, Moore TE, Grove M, Gastil RG, Ortega-Rivera A, Fanning CM. Forearc-basin sedimentary response to rapid Late Cretaceous batholith emplacement in the Peninsular Ranges of southern and Baja California. Geology. 2001 Jun 1;29(6):491-4.

Knoll AH. Life on a young planet: the first three billion years of evolution on earth. Princeton University Press; 2015 Mar 22.

Langmuir CH, Bender JF, Bence AE, Hanson GN, Taylor SR. Petrogenesis of basalts from the FAMOUS area: Mid-Atlantic Ridge. Earth and Planetary Science Letters. 1977 Aug 1;36(1):133-56.

Le Bas M, Le Maitre R, Streckeisen A, Zanettin B, IUGS Subcommission on the Systematics of Igneous Rocks. A chemical classification of volcanic rocks based on the total alkali-silica diagram. Journal of petrology. 1986 Jun 1;27(3):745-50.

Li C, Guo F, Fan W, Gao X. Ar-Ar geochronology of Late Mesozoic volcanic rocks from the Yanji area, NE China and tectonic implications. Science in China Series D: Earth Sciences. 2007 Apr 1;50(4):505-18.

Liu D, Huang Q, Fan S, Zhang L, Shi R, Ding L. Subduction of the Bangong–Nujiang Ocean: constraints from granites in the Bangong Co area, Tibet. Geological Journal. 2014 Mar;49(2):188-206.

Liu X, Xu J, Castillo PR, Xiao W, Shi Y, Feng Z, Guo L. The Dupal isotopic anomaly in the southern Paleo-Asian Ocean: Nd–Pb isotope evidence from ophiolites in Northwest China. Lithos. 2014 Feb 15;189:185-200.

Liu X, Liu W. Source characteristics and tectonic setting of the Early and Middle Devonian volcanic rocks in the North Junggar, Northwest China: Insights from Nd–Sr isotopes and geochemistry. Lithos. 2014 Jan 1;184:27-41.

Lonsdale P. Structural patterns of the Pacific floor offshore of peninsular California. The gulf and peninsular province of the Californias. 1991;47:87-125.

López-Escobar L, Cembrano J, Moreno H. Geochemistry and tectonics of the Chilean Southern Andes basaltic Quaternary volcanism (37-46 S). Andean geology. 1995 Dec 1;22(2):219-34.

Louvel M, Sanchez-Valle C, Malfait WJ, Cardon H, Testemale D, Hazemann JL. Constraints on the mobilization of Zr in magmatic-hydrothermal processes in subduction zones from in situ fluid-melt partitioning experiments. American Mineralogist. 2014 Aug 1;99(8-9):1616-25.

Luhr JF, Aranda-Gómez JJ, Housh TB. San Quintín volcanic field, Baja California Norte, México: geology, petrology, and geochemistry. Journal of Geophysical Research: Solid Earth. 1995 Jun 10;100(B6):10353-80.

Macpherson CG, Dreher ST, Thirlwall MF. Adakites without slab melting: high pressure differentiation of island arc magma, Mindanao, the Philippines. Earth and Planetary Science Letters. 2006 Mar 30;243(3):581-93.

Manikyamba C, Kerrich R, Khanna TC, Subba Rao DV. Geochemistry of adakites and rhyolites from the Neoarchaean Gadwal greenstone belt, eastern Dharwar craton, India: implications for sources and geodynamic setting. Canadian Journal of Earth Sciences. 2007 Nov 1;44(11):1517-35.

Manikyamba C, Kerrich R, Khanna TC, Krishna AK, Satyanarayanan M. Geochemical systematics of komatiite–tholeiite and adakitic-arc basalt associations: the role of a mantle plume and convergent margin in formation of the Sandur Superterrane, Dharwar craton, India. Lithos. 2008 Nov 30;106(1):155-72.

Manikyamba C, Kerrich R, Khanna TC, Satyanarayanan M, Krishna AK. Enriched and depleted arc basalts, with Mg-andesites and adakites: a potential paired arc–back-arc of the 2.6 Ga Hutti greenstone terrane, India. Geochimica et Cosmochimica Acta. 2009 Mar 15;73(6):1711-36.

Mao Q, Xiao W, Fang T, Wang J, Han C, Sun M, Yuan C. Late Ordovician to early Devonian adakites and Nb-enriched basalts in the Liuyuan area, Beishan, NW China: implications for early Paleozoic slab-melting and crustal growth in the southern Altaids. Gondwana Research. 2012 Sep 1;22(2):534-53.

Martin H. The Archean grey gneisses and the genesis of continental crust. InDevelopments in Precambrian geology 1994 Jan 1 (Vol. 11, pp. 205-259). Elsevier.

Martin H, Smithies RH, Rapp R, Moyen JF, Champion D. An overview of adakite, tonalite–trondhjemite–granodiorite (TTG), and sanukitoid: relationships and some implications for crustal evolution. Lithos. 2005 Jan 1;79(1-2):1-24.

Martin H, Moyen JF, Rapp R. The sanukitoid series: magmatism at the Archaean–Proterozoic transition. Earth and Environmental Science Transactions of the Royal Society of Edinburgh. 2009 Mar;100(1-2):15-33.

McCulloch MT, Gamble JA. Geochemical and geodynamical constraints on subduction zone magmatism. Earth and Planetary Science Letters. 1991 Mar 1;102(3-4):358-74.

McDonough WF, Sun SS. The composition of the Earth. Chemical geology. 1995 Mar 1;120(3-4):223-53.

McLennan SM, Taylor SR. Geochemical constraints on the growth of the continental crust. The Journal of Geology. 1982 Jul 1;90(4):347-61.

Miyashiro A. Volcanic rock series in island arcs and active continental margins. Amer. Jour. Sci.. 1974;274:321-55.

Motoki A, Orihashi Y, Naranjo JA, Hirata D, Skvarca P, Anma R. Geologic reconnaissance of Lautaro Volcano, Chilean Patagonia. Revista geológica de Chile. 2006 Jan;33(1):177-87.

Nauret F, Hémond C, Maury RC, Aguillon-Robles A, Guillou H, Le Faouder A. Extreme 230Th excesses in magnesian andesites from Baja California. Lithos. 2012 Aug 1;146:143-51.

Naqvi SM, Khan RM, Manikyamba C, Mohan MR, Khanna TC. Geochemistry of the NeoArchaean high-Mg basalts, boninites and adakites from the Kushtagi–Hungund greenstone belt of the Eastern Dharwar Craton (EDC); implications for the tectonic setting. Journal of Asian Earth Sciences. 2006 Jun 30;27(1):25-44.

Naqvi SM, Prathap JR. Geochemistry of adakites from Neoarchaean active continental margin of Shimoga schist belt, Western Dharwar craton, India: Implications for the genesis of TTG. Precambrian Research. 2007 Jun 20;156(1-2):32-54.

Naqvi SM, Sarma DS, Sawkar RH, Mohan MR, Prathap JR. Role of adakitic magmatism and subduction in gold endowment of Dharwar Neoarchaean greenstone belts, India. JOURNAL-GEOLOGICAL SOCIETY OF INDIA. 2008 Jun 1;71(6):875.

Negrete-Aranda R, Cañón-Tapia E, Brandle JL, Ortega-Rivera MA, Lee JK, Spelz RM, Hinojosa-Corona A. Regional orientation of tectonic stress and the stress expressed by post-subduction high-magnesium volcanism in northern Baja California, Mexico: Tectonics and volcanism of San Borja volcanic field. Journal of Volcanology and Geothermal Research. 2010 Apr 20;192(1-2):97-115.

Negrete-Aranda R, Contreras J, Spelz RM. Viscous dissipation, slab melting, and post-subduction volcanism in south-central Baja California, Mexico. Geosphere. 2013 Dec 1;9(6):1714-28.

Niu H, Sato H, Zhang H, Ito JI, Yu X, Nagao T, Terada K, Zhang Q. Juxtaposition of adakite, boninite, high-TiO 2 and low-TiO 2 basalts in the Devonian southern Altay, Xinjiang, NW China. Journal of Asian Earth Sciences. 2006 Dec 15;28(4):439-56.

Palomo AG, Macıas JL, Espındola JM. Strike-slip faults and K-alkaline volcanism at El Chichón volcano, southeastern Mexico. Journal of Volcanology and Geothermal Research. 2004 Sep 15;136(3):247-68.

Pallares C, Maury RC, Bellon H, Royer JY, Calmus T, Aguillón-Robles A, Cotten J, Benoit M, Michaud F, Bourgois J. Slab-tearing following ridge-trench collision: Evidence from Miocene volcanism in Baja California, México. Journal of Volcanology and Geothermal Research. 2007 Mar 1;161(1):95-117.

Pallares C, Bellon H, Benoit M, Maury RC, Aguillón-Robles A, Calmus T, Cotten J. Temporal geochemical evolution of Neogene volcanism in northern Baja California (27–30 N): Insights on the origin of post-subduction magnesian andesites. Lithos. 2008 Sep 1;105(1-2):162-80.

Patchett PJ, Kouvo O, Hedge CE, Tatsumoto M. Evolution of continental crust and mantle heterogeneity: evidence from Hf isotopes. Contributions to Mineralogy and Petrology. 1982 Jan 1;78(3):279-97.

Pearce JA, Cann JR. Tectonic setting of basic volcanic rocks determined using trace element analyses. Earth and planetary science letters. 1973 Jun 1;19(2):290-300.

Pearce JA, Harris NB, Tindle AG. Trace element discrimination diagrams for the tectonic interpretation of granitic rocks. Journal of petrology. 1984 Nov 1;25(4):956-83.

Pearce J. Sources and settings of granitic rocks. Episodes. 1996 Dec 1;19:120-5.

Peccerillo A, Taylor SR. Geochemistry of Eocene calc-alkaline volcanic rocks from the Kastamonu area, northern Turkey. Contributions to mineralogy and petrology. 1976 Jan 1;58(1):63-81.

Pe-Piper G, Christofides G, Eleftheriadis G. Lead and neodymium isotopic composition of Tertiary igneous rocks of northern Greece and their regional significance. Acta Vulcanologica. 1998;10:255-64.

Plank T, Langmuir CH. The chemical composition of subducting sediment and its consequences for the crust and mantle. Chemical geology. 1998 Apr 15;145(3):325-94.

Polat A, Kerrich R. Archean greenstone belt magmatism and the continental growth–mantle evolution connection: constraints from Th–U–Nb–LREE systematics of the 2.7 Ga Wawa subprovince, Superior Province, Canada. Earth and Planetary Science Letters. 2000 Jan 30;175(1):41-54.

Polat A, Münker C. Hf–Nd isotope evidence for contemporaneous subduction processes in the source of late Archean arc lavas from the Superior Province, Canada. Chemical Geology. 2004 Dec 30;213(4):403-29.

Polat A. Growth of Archean continental crust in oceanic island arcs. Geology. 2012 Apr 1;40(4):383.

Prouteau G, Maury RC, Rangin C, Suparka E, Bellon H, Pubellier M, Cotten J. Miocene adakites from northwest Borneo and their relation to the subduction of the Proto South China Sea. COMPTES RENDUS DE L ACADEMIE DES SCIENCES SERIE II FASCICULE A-SCIENCES DE LA TERRE ET DES PLANETES. 1996 Dec 2;323(11):925-32.

Prouteau G, Maury RC, Sajona FG, Cotten J, Cotten J. Behavior of niobium, tantalum and other high field strength elements in adakites and related lavas from the Philippines. Island Arc. 2000 Dec;9(4):487-98.

Puchtel IS, Hofmann AW, Amelin YV, Garbe-Schönberg CD, Samsonov AV, Shchipansky AA. Combined mantle plume-island arc model for the formation of the 2.9 Ga Sumozero-Kenozero greenstone belt, SE Baltic Shield: Isotope and trace element constraints. Geochimica et Cosmochimica Acta. 1999 Nov 30;63(21):3579-95.

Rapp RP, Shimizu N, Norman MD, Applegate GS. Reaction between slab-derived melts and peridotite in the mantle wedge: experimental constraints at 3.8 GPa. Chemical Geology. 1999 Sep 2;160(4):335-56.

Rapp RP, Shimizu N, Norman MD. Growth of early continental crust by partial melting of eclogite. Nature. 2003 Oct;425(6958):605.

Reay A, Parkinson D. Adakites from Solander Island, New Zealand. New Zealand Journal of Geology and Geophysics. 1997 Jun 1;40(2):121-6.

Rogers G, Saunders AD, Terrell DJ, Verma SP, Marriner GF. Geochemistry of Holocene volcanic rocks associated with ridge subduction in Baja California, Mexico. Nature. 1985 May;315(6018):389.

Rudnick RL. Making continental crust. Nature. 1995 Dec;378(6557):571.

Rudnick RL, Gao S. The Crust, Treatise on Geochemistry, Vol. 3. 2003.

Sajona FG, Maury RC, Bellon H, Cotten J, Defant MJ, Pubellier M. Initiation of subduction and the generation of slab melts in western and eastern Mindanao, Philippines. Geology. 1993 Nov 1;21(11):1007-10.

Sajona FG, Maury RC, Bellon H, Cotten J, Defant M. High Field Strength Element Enrichment of Pliocene—Pleistocene Island Arc Basalts, Zamboanga Peninsula, Western Mindanao (Philippines). Journal of Petrology. 1996 Jun;37(3):693-726.

Sajona FG, Bellon H, Maury RC, Pubellier M, Quebral RD, Cotten J, Bayon FE, Pagado E, Pamatian P. Tertiary and quaternary magmatism in Mindanao andLeyte (Philippines): geochronology, geochemistry and tectonic setting. Journal of Asian Earth Sciences. 1997 Jan 1;15(2-3):121-53.

Saunders AD, Rogers G, Marriner GF, Terrell DJ, Verma SP. Geochemistry of Cenezoic volcanic rocks, Baja California, Mexico: implications for the petrogenesis of post-subduction magmas. Journal of Volcanology and Geothermal Research. 1987 Jun 1;32(1-3):223-45.

Sawlan MG and Smith JG. Petrologic characteristics, age and tectonic setting of Neogene volcanic rocks in northern Baja California Sur, Mexico. (1984): 237-252.

Sawyer EW. Melt segregation in the continental crust. Geology. 1994 Nov 1;22(11):1019-22.

Shimoda G, Tatsumi Y, Nohda S, Ishizaka K, Jahn BM. Setouchi high-Mg andesites revisited: geochemical evidence for melting of subducting sediments. Earth and Planetary Science Letters. 1998 Aug 31;160(3):479-92.

Shirey SB, Hanson GN. Mantle-derived Archaean monozodiorites and trachyandesites. Nature. 1984 Jul;310(5974):222.

Silver LT, Chappell BW. The Peninsular Ranges Batholith: an insight into the evolution of the Cordilleran batholiths of southwestern North America. Earth and Environmental Science Transactions of The Royal Society of Edinburgh. 1988 Jan;79(2-3):105-21.

Singer BS, Leeman WP, Thirlwall MF, Rogers NW. Does fracture zone subduction increase sediment flux and mantle melting in subduction zones? Trace element evidence from Aleutian arc basalt. American Geophysical Union (AGU); 1996 Jan 1.

Smith, DB. U.S. Geological Survey Certificate of Analysis: Andesite, AGV-1. Denver, CO: USGS, Mar. 1995. Web page.

Smithies, RH, Champion DC, and Cassidy KF. Formation of Earth's early Archaean continental crust. Precambrian Research 127.1 (2003): 89-101.

Sohn, RA. A method for inverting ratio–ratio data to estimate end-member compositions in mixing problems. Chemical Geology 352 (2013): 63-69.

Spencer JE and Normark WR. Tosco-Abreojos fault zone: A Neogene transform plate boundary within the Pacific margin of southern Baja California, Mexico. Geology 7.11 (1979): 554-557.

Stern RA, Hanson GN, and Shirey SB. Petrogenesis of mantle-derived, LILE-enriched Archaean monzodiorites and trachyandesites (sanukitoids) in southwestern Superior Province. Canadian Journal of Earth Sciences 26.9 (1989): 1688-1712.

Stern CR, Kilian R. Role of the subducted slab, mantle wedge and continental crust in the generation of adakites from the Andean Austral Volcanic Zone. Contributions to mineralogy and petrology. 1996 Apr 1;123(3):263-81.

Storey M, Rogers G, Saunders AD, Terrell DJ. San Quintín volcanic field, Baja California, Mexico:'within-plate'magmatism following ridge subduction. Terra Nova. 1989 Mar;1(2):195-202.

Straub SM, Zellmer GF. Volcanic arcs as archives of plate tectonic change. Gondwana Research. 2012 Mar 1;21(2-3):495-516.

Streck MJ, Leeman WP, Chesley J. High-magnesian andesite from Mount Shasta: A product of magma mixing and contamination, not a primitive mantle melt. Geology. 2007 Apr 1;35(4):351-4.

Svetov SA, Huhma H, Svetova AI, Nazarova TN. The oldest adakites of the Fennoscandian Shield. In Doklady Earth Sciences C/C of Doklady-Akademia Nauk 2004 Jul 1 (Vol. 397, pp. 878-882). Interperiodica Publishing.

Tardy M, Lapierre H, Freydier C, Coulon C, Gill JB, De Lepinay BM, Beck C, Stein G, Bourdier JL, Yta M. The Guerrero suspect terrane (western Mexico) and coeval arc terranes (the Greater Antilles and the Western Cordillera of Colombia): A late Mesozoic intra-oceanic arc accreted to cratonal America during the Cretaceous. Tectonophysics. 1994 Feb 15;230(1-2):49-73.

Tatsumi Y, Kogiso T. Trace element transport during dehydration processes in the subducted oceanic crust: 2. Origin of chemical and physical characteristics in arc magmatism. Earth and Planetary Science Letters. 1997 Apr 1;148(1-2):207-21.

Tatsumi Y, Shukuno H, Yoshikawa M, Chang Q, Sato K, Lee MW. The petrology and geochemistry of volcanic rocks on Jeju Island: plume magmatism along the Asian continental margin. Journal of Petrology. 2004 Nov 24;46(3):523-53.

Tatsumi Y. High-Mg andesites in the Setouchi volcanic belt, southwestern Japan: analogy to Archean magmatism and continental crust formation?. Annu. Rev. Earth. Planet. Sci.. 2006 May 30;34:467-99.

Tatsumi Y, Shukuno H, Tani K, Takahashi N, Kodaira S, Kogiso T. Structure and growth of the Izu-Bonin-Mariana arc crust: 2. Role of crust-mantle transformation and the transparent Moho in arc crust evolution. Journal of Geophysical Research: Solid Earth. 2008 Feb 1;113(B2).

TaylorSR, McLennanSM. "The continental crust: its composition and evolution." BlackwellScientific Publications (1985): 1-328.

Taylor SR, McLennan SM. The geochemical evolution of the continental crust. Reviews of Geophysics. 1995 May;33(2):241-65.

Tian L, Castillo PR, Lonsdale PF, Hahm D, Hilton DR. Petrology and Sr-Nd-Pb-He isotope geochemistry of postspreading lavas on fossil spreading axes off Baja California Sur, Mexico. Geochemistry, Geophysics, Geosystems. 2011 Feb 1;12(2).

Todd VR, Kimbrough DL, Herzig CT. The Peninsular Ranges batholith from western arc to eastern mid-crustal intrusive and metamorphic rocks. San Diego County, California: Geological Society of America Fieldtrip Guidebook, Cordilleran Section, San Bernardino, California. 1994:235-40.

Tokunaga S, Nakai SI, Orihashi Y. Two types of adakites revealed by 238U-230Th disequilibrium from Daisen Volcano, southwestern Japan. Geochemical Journal. 2010 Oct 20;44(5):379-86.

Ujike O, Goodwin AM, Shibata T. Geochemistry and origin of Archean volcanic rocks from the Upper Keewatin assemblage (ca 2.7 Ga), Lake of the Woods greenstone belt, western Wabigoon Subprovince, Superior Province, Canada. Island Arc. 2007 Mar;16(1):191-208.

Umhoefer PJ. A model for the North America Cordillera in the Early Cretaceous: Tectonic escape related to arc collision of the Guerrero terrane and a change in North America plate motion. SPECIAL PAPERS-GEOLOGICAL SOCIETY OF AMERICA. 2003 Jan 1:117-34.

Valley JW, Cavosie AJ, Ushikubo T, Reinhard DA, Lawrence DF, Larson DJ, Clifton PH, Kelly TF, Wilde SA, Moser DE, Spicuzza MJ. Hadean age for a post-magma-ocean zircon confirmed by atom-probe tomography. Nature Geoscience. 2014 Mar 1;7(3):219-23.

Verma SP. Alkali and alkaline earth element geochemistry of Los Humeros Caldera, Puebla, Mexico. Journal of volcanology and geothermal research. 1984 Mar 1;20(1-2):21-40.

Verma SP, Nelson SA. Isotopic and trace element constraints on the origin and evolution of alkaline and calc-alkaline magmas in the Northwestern Mexican Volcanic Belt. Journal of Geophysical Research: Solid Earth. 1989 Apr 10;94(B4):4531-44.

Verma SP, Carrasco-N'uñez G, Milán M. Geology and geochemistry of Amealco caldera, Qro., Mexico. Journal of Volcanology and Geothermal Research. 1991 Jul 1;47(1-2):105-27.

Verma SP. Geochemical evidence for a lithospheric source for magmas from Los Humeros caldera, Puebla, Mexico. Chemical Geology. 2000 Mar 6;164(1):35-60.

Verma SP. Geochemical and Sr–Nd–Pb isotopic evidence for a combined assimilation and fractional crystallisation process for volcanic rocks from the Huichapan caldera, Hidalgo, Mexico. Lithos. 2001 Mar 31;56(2):141-64.

Wallace P, Carmichael IS. Sulfur in basaltic magmas. Geochimica et Cosmochimica Acta. 1992 May 1;56(5):1863-74.

Wang Q, Wyman DA, Xu J, Dong Y, Vasconcelos PM, Pearson N, Wan Y, Dong H, Li C, Yu Y, Zhu T. Eocene melting of subducting continental crust and early uplifting of central Tibet: evidence from central-western Qiangtang high-K calc-alkaline andesites, dacites and rhyolites. Earth and Planetary Science Letters. 2008 Jul 30;272(1):158-71.

Wang Y, Cheng SH. Field relation, geochemistry and origin of the Xinglonggou volcanic rocks in Beipiao area, Liaoning Province (China): Reappraisal on the foundering of lower continental crust of North China Craton. Journal of Asian Earth Sciences. 2012 Mar 30;47:35-50.

Wang Y, Forsyth DW, Savage B. Convective upwelling in the mantle beneath the Gulf of California. Nature. 2009 Nov;462(7272):499.

Wang XL, Jiang SY, Dai BZ. Melting of enriched Archean subcontinental lithospheric mantle: Evidence from the ca. 1760Ma volcanic rocks of the Xiong'er Group, southern margin of the North China Craton. Precambrian Research. 2010 Oct 1;182(3):204-16.

Warren JM. Global variations in abyssal peridotite compositions. Lithos. 2016 Apr 1;248:193-219.

Wilson BM. Igneous petrogenesis a global tectonic approach. Springer Science & Business Media; 2007 Sep 23.

Winchester JA, Floyd PA. Geochemical discrimination of different magma series and their differentiation products using immobile elements. Chemical geology. 1977 Jan 1;20:325-43.

Woodhead JD, Eggins SM, Johnson RW. Magma genesis in the New Britain island arc: further insights into melting and mass transfer processes. Journal of Petrology. 1998 Sep 1;39(9):1641-68.

Workman RK, Hart SR. Major and trace element composition of the depleted MORB mantle (DMM). Earth and Planetary Science Letters. 2005 Feb 28;231(1):53-72.

Xiong XL, Zhao ZH, Bai ZH, Mei HJ, Xu JF, Wang Q. Origin of Awulale adakitic sodium-rich rocks in western Tianshan: Constraints for Nd and Sr isotopic compositions. Acta Petrologica Sinica. 2001 Oct 1;17(4):514-22.

Yamamoto T, Hoang N. Synchronous Japan Sea opening Miocene fore-arc volcanism in the Abukuma Mountains, NE Japan: An advancing hot asthenosphere flow versus Pacific slab melting. Lithos. 2009 Oct 31;112(3):575-90.

Yogodzinski GM, Kelemen PB. Slab melting in the Aleutians: implications of an ion probe study of clinopyroxene in primitive adakite and basalt. Earth and Planetary Science Letters. 1998 May 15;158(1-2):53-65.

You CF, Castillo PR, Gieskes JM, Chan LH, Spivack AJ. Trace element behavior in hydrothermal experiments: Implications for fluid processes at shallow depths in subduction zones. Earth and Planetary Science Letters. 1996 May 1;140(1-4):41-52.

Zhang H, Niu H, Sato H, Yu X, Shan Q, Zhang B, Ito JI, Nagao T. Late Paleozoic adakites and Nb-enriched basalts from northern Xinjiang, northwest China: Evidence for the southward subduction of the Paleo-Asian Oceanic Plate. Island Arc. 2005 Mar;14(1):55-68.

Zhang YB, Sun SH, Mao Q. Mesozoic O-type adakitic volcanic rocks and its petrogenesis, paleo-tectonic dynamic and mineralization significance of the eastern side of southern Da Hinggan, China. Acta Petrologica Sinica. 2006;22:2289-304.

Zhao ZH, Xiong XL, Wang Q, Wyman DA, Bao ZW, Bai ZH, Qiao YL. Underplating-related adakites in Xinjiang Tianshan, China. Lithos. 2008 Apr 30;102(1):374-91.